

Ultralight scalars in leptonic observables

Pablo Escribano^a, Avelino Vicente^{a,b}

- (a) Instituto de Física Corpuscular, CSIC-Universitat de València, 46980 Paterna, Spain
(b) Departament de Física Teòrica, Universitat de València, 46100 Burjassot, Spain

pablo.escribano@ific.uv.es, avelino.vicente@ific.uv.es

Abstract

Many new physics scenarios contain ultralight scalars, states which are either exactly massless or much lighter than any other massive particle in the model. Axions and majorons constitute well-motivated examples of this type of particle. In this work, we explore the phenomenology of these states in low-energy leptonic observables. After adopting a model independent approach that includes both scalar and pseudoscalar interactions, we briefly discuss the current limits on the diagonal couplings to charged leptons and consider processes in which the ultralight scalar ϕ is directly produced, such as $\mu \rightarrow e \phi$, or acts as a mediator, as in $\tau \rightarrow \mu\mu\mu$. Contributions to the charged leptons anomalous magnetic moments are studied as well.

Contents

| | | |
|----------|--------------------------------------------------------------------------------|-----------|
| 1 | Introduction | 3 |
| 2 | Effective Lagrangian | 4 |
| 3 | Bounds on lepton flavor conserving couplings | 5 |
| 3.1 | Stellar cooling | 6 |
| 3.2 | 1-loop coupling to photons | 7 |
| 4 | Leptonic observables | 9 |
| 4.1 | $\ell_\alpha \rightarrow \ell_\beta \phi$ | 9 |
| 4.2 | $\ell_\alpha \rightarrow \ell_\beta \gamma \phi$ | 11 |
| 4.3 | $\ell_\alpha^- \rightarrow \ell_\beta^- \ell_\beta^- \ell_\beta^+$ | 14 |
| 4.4 | $\ell_\alpha^- \rightarrow \ell_\beta^- \ell_\gamma^- \ell_\gamma^+$ | 16 |
| 4.5 | $\ell_\alpha^- \rightarrow \ell_\beta^+ \ell_\gamma^- \ell_\gamma^-$ | 17 |
| 4.6 | Lepton anomalous magnetic moments | 18 |
| 5 | Conclusions | 20 |
| A | Parametrization in terms of derivative interactions | 21 |

1 Introduction

Lepton flavor physics is about to live a golden age. Several state-of-the-art experiments recently started taking data and a few more are about to begin [1]. These include new searches for lepton flavor violating (LFV) processes, forbidden in the Standard Model (SM), as well as more precise measurements of lepton flavor conserving observables, such as charged lepton anomalous magnetic moments. The search for LFV in processes involving charged leptons is strongly motivated by the observation of LFV in the neutral sector (in the form of neutrino flavor oscillations). In what concerns muon observables, the search for the radiative LFV decay $\mu \rightarrow e\gamma$ is going to be led by the second phase of the MEG experiment, MEG-II [2, 3], while the long-awaited Mu3e experiment will aim at an impressive sensitivity to branching ratios for the 3-body decay $\mu \rightarrow eee$ as low as 10^{-16} [3, 4]. A plethora of promising experiments looking for neutrinoless $\mu - e$ conversion in nuclei is also planned. Flavor factories and experiments aiming at a broad spectrum of flavor observables, such as Belle II and LHCb, will also contribute to this era of lepton flavor, mainly due to their high sensitivities in the measurement of tau lepton observables [5, 6]. On the flavor conserving side, improved measurements of the muon anomalous magnetic moment are expected at the Muon g-2 experiment [7], hopefully shedding light on a well-known long-standing experimental anomaly.

With such an exciting experimental perspective in the coming years, it is natural to ask what type of new physics can be probed. In this work we will concentrate on ultralight scalars that couple to charged leptons and study their impact on leptonic observables. In this context, we will use the term *ultralight scalar* to refer to a generic scalar ϕ that is much lighter than the electron, $m_\phi \ll m_e$, and can therefore be produced on-shell in charged lepton decays. In practice, this also means that ϕ can be assumed to be approximately massless in all considered physical processes. We will take a model independent approach and neglect m_ϕ in our analytical calculations. Actually, this is not an approximation if ϕ is exactly massless, the case for a Goldstone boson whose mass is protected by a (spontaneously broken) global continuous symmetry.

There are many well-known examples of such ultralight scalars. If the apparent absence of CP violation in the strong interactions is explained by means of the Peccei-Quinn mechanism [8], a new pseudoscalar state must exist: the axion [9, 10]. Although its mass is not predicted and can vary over a wide range of scales [11], a large fraction of the parameter space (corresponding to large axion decay constants) leads to an ultralight axion. Interestingly, such low mass axion would be of interest as a possible component of the dark matter of the Universe [12–14]. Axion-like particles, or ALPs, generalize this type of scenario by making the mass and decay constant two independent parameters. This allows for a larger parameter space, again including a substantial portion with very low ALP masses. The solution to the strong CP problem could also be intimately related to the flavor problem of the SM [15]. This naturally leads to a flavored axion [16–18], although an axion with flavor-blind interactions is also possible [19]. Another popular ultralight scalar is the majoron, the Goldstone boson associated to the breaking of global lepton number [20–23]. While this state can gain a small mass by various mechanisms, and then be a possible dark matter candidate [24, 25], it is expected to be exactly massless in the absence of explicit breaking of lepton number. Another possible ultralight scalar is the familon, the Goldstone boson

of spontaneously broken global family symmetry. Finally, the Universe could also be filled with ultralight scalars in the form of fuzzy cold dark matter [26].

While many of the previously discussed examples are pseudoscalar states, the ultralight scalar ϕ can also have pure scalar couplings. This would be the case for a massless Goldstone boson if the associated global symmetry is non-chiral. Therefore, restricting the phenomenological exploration to just pseudoscalars would miss a relatively large number of well-motivated scenarios. This has actually been the case in many recent works [27–35], which were mainly interested in the phenomenology of flavored axions (or ALPs) and majorons [36].

Motivated by the principle of generality, we will consider a generic scenario where the CP nature of ϕ is not determined and explore several leptonic observables of interest. These include processes in which ϕ is produced in the final state, such as $\ell_\alpha \rightarrow \ell_\beta \phi$ or $\ell_\alpha \rightarrow \ell_\beta \phi \gamma$. In this case, we will generalize previous results in the literature, typically obtained for pure pseudoscalars or for the case of a massive ϕ . We will also study processes in which ϕ is not produced, but acts as a mediator. A prime example of this category is $\ell_\alpha^- \rightarrow \ell_\beta^- \ell_\beta^- \ell_\beta^+$. To the best of our knowledge, the mediation of this process by an ultralight axion has only been previously considered in [27]. We will extend the study to more general scalar states and provide detailed analytical expressions for the decay width of the process. The analogous $\ell_\alpha^- \rightarrow \ell_\beta^- \ell_\gamma^- \ell_\gamma^+$ and $\ell_\alpha^- \rightarrow \ell_\beta^+ \ell_\gamma^- \ell_\gamma^-$ decays will also be studied, in this case for the first time here. Charged lepton anomalous magnetic moments constitute other interesting examples of observables induced by the ultralight ϕ .

The rest of the manuscript is organized as follows. We introduce our general setup, as well as our notation and conventions, in Sec. 2. In Sec. 3 we discuss the current bounds on the lepton flavor conserving couplings of the scalar ϕ . These are often constrained by studying their impact on astrophysical processes, but also receive indirect bounds due to their contribution to the 1-loop coupling of ϕ to photons, as we will show. Sec. 4 contains the main results of this work. In this Section we discuss the impact of ϕ on several leptonic observables and consider the phenomenological implications. We summarize our findings and conclude in Sec. 5. Finally, a pedagogical discussion on an alternative parametrization of the ϕ Lagrangian in terms of derivative interactions is provided in Appendix A.

2 Effective Lagrangian

We are interested in charged leptons processes taking place at low energies in the presence of the ultralight real scalar ϕ . For practical purposes, we will consider ϕ to be exactly massless, but our results are equally valid for a massive ϕ , as long as $m_\phi \ll m_e$ holds. The interaction of the scalar ϕ with a pair of charged leptons ℓ_α and ℓ_β , with $\alpha, \beta = e, \mu, \tau$, can be generally parametrized by

$$\mathcal{L}_{\ell\ell\phi} = \phi \bar{\ell}_\beta (S_L P_L + S_R P_R) \ell_\alpha + \text{h.c.}, \quad (1)$$

where $P_{L,R} = \frac{1}{2}(1 \mp \gamma_5)$ are the usual chiral projectors. No sum over the α and β charged lepton flavor indices is performed. The dimensionless coefficients S_L and S_R are 3×3 matrices carrying flavor indices, omitted to simplify the notation. Eq. (1) describes the most general effective interaction between the ultralight scalar ϕ and a pair of charged leptons. In particular, we note that Eq. (1) includes both scalar and pseudoscalar interactions. An

alternative parametrization for this Lagrangian based on the introduction of derivative interactions, applicable to the case of pseudoscalar interactions only, is discussed in Appendix A. Finally, Eq. (1) includes flavor violating (charged lepton fields with $\alpha \neq \beta$) as well as flavor conserving (charged lepton fields with $\alpha = \beta$) interactions.

Some of the LFV observables considered below receive contributions from the usual dipole and 4-fermion operators. Therefore, our full effective Lagrangian is given by

$$\mathcal{L} = \mathcal{L}_{\ell\ell\phi} + \mathcal{L}_{\ell\ell\gamma} + \mathcal{L}_{4\ell}, \quad (2)$$

with

$$\mathcal{L}_{\ell\ell\gamma} = \frac{e m_\alpha}{2} \bar{\ell}_\beta \sigma^{\mu\nu} (K_2^L P_L + K_2^R P_R) \ell_\alpha F_{\mu\nu} + \text{h.c.}, \quad (3)$$

$$\mathcal{L}_{4\ell} = \sum_{\substack{I=S,V,T \\ X,Y=L,R}} A_{XY}^I \bar{\ell}_\beta \Gamma_I P_X \ell_\alpha \bar{\ell}_\delta \Gamma_I P_Y \ell_\gamma + \text{h.c.}, \quad (4)$$

where $F_{\mu\nu} = \partial_\mu A_\nu - \partial_\nu A_\mu$ is the electromagnetic field strength tensor, with A_μ the photon field, and we have defined $\Gamma_S = 1$, $\Gamma_V = \gamma_\mu$ and $\Gamma_T = \sigma_{\mu\nu}$. No sum over the α, β, γ and δ charged lepton flavor indices is performed in Eqs. (3) and (4). The coefficients K_2^X and A_{XY}^I , with $I = S, V, T$ and $X, Y = L, R$, carry flavor indices, again omitted to simplify the notation, and have dimensions of mass^{-2} . We assume $m_\alpha > m_\beta$ and therefore normalize the Lagrangian in Eq. (3) by including the mass of the heaviest charged lepton in the process of interest. Eq. (3) contains the usual photonic dipole operators, which contribute to $\ell_\alpha \rightarrow \ell_\beta \gamma$ and lead to

$$\Gamma(\ell_\alpha \rightarrow \ell_\beta \gamma) = \frac{e^2 m_\alpha^5}{16 \pi} (|K_2^L|^2 + |K_2^R|^2), \quad (5)$$

while Eq. (4) contains 4-lepton operators. In summary, the effective Lagrangian in Eq. (2) corresponds to the one in [37], extended to include the new operators with the scalar ϕ introduced in Eq. (1).

In the following, we will disregard ϕ interactions with quarks and concentrate on purely leptonic observables, such as the LFV decays $\ell_\alpha \rightarrow \ell_\beta \phi$ or $\ell_\alpha \rightarrow \ell_\beta \ell_\beta \ell_\beta$, and the electron and muon anomalous magnetic dipole moments. Even though ϕ couplings to quarks are possible, and indeed present in specific realizations of our general scenario, the prime example being the QCD axion, they introduce a large model dependence. We also note that leptophilic ultralight scalars, such as the majoron, are also well-motivated possibilities that naturally appear in models with spontaneous violation of global lepton number.

3 Bounds on lepton flavor conserving couplings

Let us comment on the current experimental constraints on the lepton flavor conserving couplings of the scalar ϕ . We will start discussing the stellar cooling mechanism. Since this subject has been extensively studied in the literature, and we do not want to delve further into the topic, only a brief outline will be presented. Then we will discuss another source of constraints, the 1-loop coupling between ϕ and a pair of photons.

3.1 Stellar cooling

The production of ϕ scalar particles inside stars, followed by their emission, may constitute a powerful stellar cooling mechanism. If this process takes place at a high rate, it may alter star evolution, eventually leading to conflict with astrophysical observations [38]. This allows one to place strong constraints on the ϕ scalar couplings. The dominant cooling mechanisms are scalar bremsstrahlung in lepton-nucleus scattering, $\ell^- + N \rightarrow \ell^- + N + \phi$, and the Compton process $\gamma + \ell^- \rightarrow \ell^- + \phi$. Their relative importance depends on the density and temperature of the medium, and therefore on the astrophysical scenario. In particular, the Compton process dominates only at low densities and high temperatures, conditions that can be found in red giants. Limits can also be derived from the production of ultralight scalars in supernovae. The scalar ϕ can be efficiently produced and, since it will typically escape without interacting with the medium, a net transport of energy out of the supernova will take place. Such a loss of energy may dramatically affect other processes taking place in the supernova, such as neutrino production.

Plenty of works have recently studied the question of cooling by the emission of ultralight scalars in astrophysical scenarios [11, 35, 39–41]. However, to the best of our knowledge, all of them consider axions or ALPs. These are low-mass pseudoscalars and thus, their impact on stellar evolution can only be used to constrain pseudoscalar couplings. Even though we will not provide a detailed calculation to support this statement, we will argue that similar bounds can be set on the scalar couplings.

To make explicit the pure scalar and pseudoscalar interactions, we can use a redefinition of our Lagrangian in Eq. (1) which, for the diagonal terms, can be written as

$$\mathcal{L}_{\ell\ell\phi}^{\text{diag}} = \phi \bar{\ell}_\beta (S P_L + S^* P_R) \ell_\beta = \phi \bar{\ell}_\beta [\text{Re } S - i \text{Im } S \gamma_5] \ell_\beta, \quad (6)$$

with $S = S_L + S_R^*$. For a pure pseudoscalar, only $\text{Im } S$ is present.

The currently most stringent limit on the pseudoscalar coupling with electrons is obtained from white dwarfs. Specifically, the limit is obtained by considering the bremsstrahlung process, which can be very efficient in the dense core of a white dwarf. Using data from the Sloan Digital Sky Survey and the SuperCOSMOS Sky Survey, Ref. [42] found (at 90% C.L.)

$$\text{Im } S^{ee} < 2.1 \times 10^{-13}. \quad (7)$$

The coupling with muons has been recently studied in some works [35, 39, 40]. In this case the process ultimately used to set the constraint is neutrino production, clearly suppressed if energy is transported out of the supernova by scalars produced in $\mu + \gamma \rightarrow \mu + \phi$. Using the famous supernova SN1987A, Ref. [40] has found

$$\text{Im } S^{\mu\mu} < 2.1 \times 10^{-10}. \quad (8)$$

Setting precise limits for the scalar parts of the couplings would imply the calculation of the cross sections and the energy-loss rates per unit mass, as required to perform a complete analysis. Instead, one can gauge the relevance of the bounds on the scalar couplings with the following arguments. First, we note that if the charged lepton mass is neglected, the scalar and pseudoscalar couplings contribute in exactly the same way to the relevant cross sections. This is, however, a bad approximation, due to the low energies involved in the astrophysical

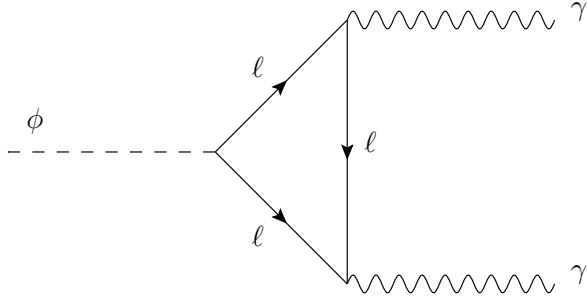


Figure 1: Loop induced coupling of ϕ to a pair of photons.

scenarios that set the limits. For this reason, one must keep the charged lepton mass. We have numerically integrated the cross sections for a wide range of low energies and found that, for the same numerical value of $\text{Re } S$ and $\text{Im } S$, the scalar interaction always gives larger cross sections. Therefore, the constraints on the scalar couplings will be stronger and we can conclude that

$$\text{Re } S^{\beta\beta} \lesssim [\text{Im } S^{\beta\beta}]_{\text{max}} , \quad (9)$$

with $\beta = e, \mu$. Nevertheless, we point out that a detailed analysis of the cooling mechanism with pure scalars is required to fully determine the corresponding bounds.

Finally, one should note that these limits are based on the (reasonable) assumption that the scalar properties are not altered in the astrophysical medium. In particular, its mass and couplings are assumed to be the same as in vacuum. Some mechanisms have been recently proposed [43, 44] (see also previous work in [45]) that would make this assumption invalid. These works are mainly motivated by the recent XENON1T results, which include a 3.5σ excess of low-energy electron recoil events [46]. An axion explaining this excess would violate the astrophysical constraints, since the required coupling to electrons would be larger than the limit in Eq. (7), see for instance [41]. This motivates the consideration of mechanisms that alter the effective couplings to electrons or the axion mass in high density scenarios. If any of these mechanisms are at work, larger diagonal couplings would be allowed. However, we note that additional bounds, not derived from astrophysical observations, can be set on the diagonal couplings. This is precisely what we proceed to discuss.

3.2 1-loop coupling to photons

The interaction of the scalar ϕ to a pair of photons is described by the effective Lagrangian

$$\mathcal{L}_{\phi\gamma\gamma} = g_{S\gamma\gamma} \phi F_{\mu\nu} F^{\mu\nu} + g_{A\gamma\gamma} \phi F_{\mu\nu} \tilde{F}^{\mu\nu} , \quad (10)$$

where $g_{S\gamma\gamma}$ and $g_{A\gamma\gamma}$ are the couplings for a pure scalar and a pure pseudoscalar, respectively, and $\tilde{F}^{\mu\nu}$ is the dual electromagnetic tensor, defined as

$$\tilde{F}^{\mu\nu} = \frac{1}{2} \varepsilon^{\mu\nu\alpha\beta} F_{\alpha\beta} . \quad (11)$$

The $g_{S\gamma\gamma}$ and $g_{A\gamma\gamma}$ couplings can be induced at the 1-loop level from diagrams involving charged leptons, as shown in Fig. 1. Since $g_{S\gamma\gamma}$ and $g_{A\gamma\gamma}$ are constrained by a variety of

experimental sources, this can be used to set indirect constraints on the ϕ couplings to charged leptons introduced in Eq. (1). In particular, we will take advantage of this relation to get additional limits on the lepton flavor conserving couplings of ϕ .

The 1-loop analytical expression for $g_{S\gamma\gamma}$ and $g_{A\gamma\gamma}$ can be written as [47]

$$|g_{I\gamma\gamma}|^2 = \frac{\alpha^2}{64\pi^2} \left| \sum_{\beta} \frac{g_{I\beta\beta}}{m_{\beta}} A_{1/2}^I(\tau_{\beta}) \right|^2, \quad (12)$$

where $I = S, A$. Here $A_{1/2}^S$ and $A_{1/2}^A$ are 1-loop fermionic functions defined as

$$A_{1/2}^S(\tau_{\beta}) = 2[\tau_{\beta} + (\tau_{\beta} - 1)f(\tau_{\beta})]\tau_{\beta}^{-2} \quad (13)$$

for the scalar coupling and

$$A_{1/2}^A(\tau_{\beta}) = 2\tau_{\beta}^{-1}f(\tau_{\beta}) \quad (14)$$

for the pseudoscalar case, with $\tau_{\beta} = m_{\phi}^2/4m_{\beta}^2$. The function $f(\tau)$ can be found for instance in [48]. It is given by

$$f(\tau) \equiv \begin{cases} \arcsin^2 \sqrt{\tau} & \tau \leq 1 \\ -\frac{1}{4} \left[\log \frac{1+\sqrt{1-\tau^{-1}}}{1-\sqrt{1-\tau^{-1}}} - i\pi \right]^2 & \tau > 1 \end{cases}. \quad (15)$$

In this work we consider the case of an ultralight scalar. In the massless limit, the loop functions reduce simply to $A_{1/2}^S(0) = \frac{4}{3}$ and $A_{1/2}^A(0) = 2$, and then we can write

$$\begin{aligned} |g_{S\gamma\gamma}|^2 &= \frac{\alpha^2}{36\pi^2} \left| \sum_{\beta} \frac{g_{S\beta\beta}}{m_{\beta}} \right|^2, \\ |g_{A\gamma\gamma}|^2 &= \frac{\alpha^2}{16\pi^2} \left| \sum_{\beta} \frac{g_{A\beta\beta}}{m_{\beta}} \right|^2, \end{aligned} \quad (16)$$

with the couplings to the charged leptons being given by

$$\begin{aligned} g_{S\beta\beta} &= \text{Re } S^{\beta\beta}, \\ g_{A\beta\beta} &= \text{Im } S^{\beta\beta}. \end{aligned} \quad (17)$$

We are now in position to compare to the current experimental limits on the coupling to photons. These are of two types. First, let us consider astrophysical limits. Magnetic fields around astrophysical sources of photons may transform these into scalars, an effect that can be used to set constraints on their coupling. Ref. [49] provides a comprehensive recollection of limits from astrophysical observations. Using results from [50], this reference finds that for scalar masses in the range $m_{\phi} \ll 1 \text{ peV} - 1 \text{ neV}$, astrophysical constraints imply

$$g_{I\gamma\gamma} \lesssim (10^{-12} - 10^{-11}) \text{ GeV}^{-1} \quad (18)$$

for both scalar and pseudoscalar couplings. Taking this into account, we can find the relations

$$\begin{aligned} \left| \sum_{\beta} \frac{\text{Re } S^{\beta\beta}}{m_{\beta}} \right|^2 &= \frac{36 \pi^2}{\alpha^2} g_{S\gamma\gamma}^2 < 6.7 \times 10^{-16} \text{ GeV}^{-2}, \\ \left| \sum_{\beta} \frac{\text{Im } S^{\beta\beta}}{m_{\beta}} \right|^2 &= \frac{16 \pi^2}{\alpha^2} g_{A\gamma\gamma}^2 < 3.0 \times 10^{-16} \text{ GeV}^{-2}, \end{aligned} \quad (19)$$

which translate into very stringent bounds on the diagonal couplings to charged leptons, $S^{ee} \lesssim 10^{-11}$ and $S^{\mu\mu} \lesssim 10^{-9}$. The OSQAR experiment [51], a light-shining-through-a-wall experiment, has also derived limits for massless scalars. Again, these are valid for both scalar and pseudoscalar couplings,

$$g_{I\gamma\gamma} < 5.76 \times 10^{-8} \text{ GeV}^{-1}, \quad (20)$$

and therefore,

$$\begin{aligned} \left| \sum_{\beta} \frac{\text{Re } S^{\beta\beta}}{m_{\beta}} \right|^2 &= \frac{36 \pi^2}{\alpha^2} g_{S\gamma\gamma}^2 < 3.8 \times 10^{-8} \text{ GeV}^{-2}, \\ \left| \sum_{\beta} \frac{\text{Im } S^{\beta\beta}}{m_{\beta}} \right|^2 &= \frac{16 \pi^2}{\alpha^2} g_{A\gamma\gamma}^2 < 1.7 \times 10^{-8} \text{ GeV}^{-2}. \end{aligned} \quad (21)$$

These relations also imply strong constraints on the diagonal couplings to charged leptons, but milder than in the previous case, $S^{ee} \lesssim 10^{-7}$ and $S^{\mu\mu} \lesssim 10^{-5}$.

Finally, we point out that these indirect limits are strictly only valid if the diagrams in Fig. 1 are the only contribution to the ϕ coupling to photons. If more contributions exist, possible cancellations among them may reduce the total coupling so that the constraints are satisfied for larger couplings to charged leptons. We should also note that astrophysical constraints are subject to the same limitation discussed above. They rely on the assumption that the properties of ϕ in the astrophysical medium are the same as in vacuum.

4 Leptonic observables

4.1 $\ell_{\alpha} \rightarrow \ell_{\beta} \phi$

The off-diagonal $S_A^{\beta\alpha}$ scalar couplings, with $A = L, R$, can be directly constrained by the LFV decays $\ell_{\alpha} \rightarrow \ell_{\beta} \phi$. Using the effective Lagrangian in Eq. (1), it is straightforward to obtain

$$\Gamma(\ell_{\alpha} \rightarrow \ell_{\beta} \phi) = \frac{m_{\alpha}}{32 \pi} \left(\left| S_L^{\beta\alpha} \right|^2 + \left| S_R^{\beta\alpha} \right|^2 \right), \quad (22)$$

where terms proportional to the small ratio m_{β}/m_{α} have been neglected.¹

¹We must notice that this approximation is not equally good for all $\ell_{\alpha} \rightarrow \ell_{\beta} \phi$ cases. This is because the ratio $m_{\mu}/m_{\tau} \sim 0.1$ is not completely negligible. Therefore, while the approximation is very good for

Several searches for $\ell_\alpha \rightarrow \ell_\beta \phi$ have been performed and used to set experimental constraints on the off-diagonal $S_A^{\beta\alpha}$ effective couplings. Let us start with muon decays. The strongest limit on the branching ratio for the 2-body decay $\mu^+ \rightarrow e^+ \phi$ was obtained at TRIUMF, finding $\text{BR}(\mu \rightarrow e \phi) < 2.6 \times 10^{-6}$ at 90% C.L. [52]. However, as explained in [53], this experimental limit must be applied with care to the general scenario considered here. The reason is that the experimental setup in [52] uses a muon beam that is highly polarized in the direction opposite to the muon momentum and concentrates the search in the forward region. This reduces the background from the SM process $\mu^+ \rightarrow e^+ \nu_e \bar{\nu}_\mu$, which is strongly suppressed in this region, but also reduces the $\mu^+ \rightarrow e^+ \phi$ signal unless the $\phi - e - \mu$ coupling is purely right-handed. Therefore, we obtain a limit valid only when $S_L^{e\mu} = 0$:

$$S_L^{e\mu} = 0 \quad \Rightarrow \quad |S_R^{e\mu}| < 2.7 \times 10^{-11}. \quad (23)$$

A more general limit can also be derived from [52]. Using the spin processed data shown in Fig.(7) of [52], the authors of [53] obtained the conservative bound $\text{BR}(\mu \rightarrow e \phi) \lesssim 10^{-5}$, valid for any chiral structure of the $S_A^{e\mu}$ couplings. This bound is similar to the more recent limit obtained by the TWIST collaboration [54], also in the $\sim 10^{-5}$ ballpark. With this value, one finds an upper limit on the $e - \mu$ flavor violating couplings of ²

$$|S^{e\mu}| < 5.3 \times 10^{-11}. \quad (24)$$

where we have defined the convenient combination

$$|S^{\beta\alpha}| = \left(|S_L^{\beta\alpha}|^2 + |S_R^{\beta\alpha}|^2 \right)^{1/2}. \quad (25)$$

Several strategies can be followed for newer $\mu \rightarrow e \phi$ searches. The authors of [35] advocate for a new phase of the MEG II experiment, reconfigured to search for $\mu \rightarrow e \phi$ by placing a Lyso calorimeter in the forward direction. Also, as pointed out in [55, 56] and recently discussed in [35] as well, the limit in Eq. (24) can be substantially improved by the Mu3e experiment by looking for a bump in the continuous Michel spectrum. The detailed analysis in [56] shows that $\mu \rightarrow e \phi$ branching ratios above 7.3×10^{-8} can be ruled out at 90% C.L.. This would imply a sensitivity to an $|S^{e\mu}|$ effective coupling as low as 4.5×10^{-12} , improving an order of magnitude with respect to the limit in Eq. (24).

Turning to τ decays, the currently best experimental limits were set by the ARGUS collaboration [57], which found

$$\begin{aligned} \frac{\text{BR}(\tau \rightarrow e \phi)}{\text{BR}(\tau \rightarrow e \nu \bar{\nu})} &< 0.015, \\ \frac{\text{BR}(\tau \rightarrow \mu \phi)}{\text{BR}(\tau \rightarrow \mu \nu \bar{\nu})} &< 0.026, \end{aligned} \quad (26)$$

$\mu \rightarrow e \phi$ and $\tau \rightarrow e \phi$, it may lead to an error of the order of 20% in $\tau \rightarrow \mu \phi$. This deviation is acceptable, but can be accounted for by including additional terms proportional to m_μ/m_τ , hence leading to a much more complicated analytical expression. Completely analogous comments can be made for the rest of the observables discussed in this Section.

²See also the recent [35] for a comprehensive discussion of the experimental limit of [52] and how this gets altered for different chiral structures of the $S_A^{e\mu}$ couplings.

at 95% C.L.. These limits are weaker than those for muon decays, but still lead to stringent constraints on the LFV τ couplings with the scalar ϕ . It is straightforward to find

$$\begin{aligned} |S^{e\tau}| &< 5.9 \times 10^{-7}, \\ |S^{\mu\tau}| &< 7.6 \times 10^{-7}. \end{aligned} \tag{27}$$

These limits for the LFV couplings to τ leptons are expected to be improved at Belle II. In fact, new methods for $\tau \rightarrow \ell \phi$ searches at this experiment have been recently proposed [58].

4.2 $\ell_\alpha \rightarrow \ell_\beta \gamma \phi$

The decay width for the 3-body LFV process $\ell_\alpha \rightarrow \ell_\beta \gamma \phi$ can be written as

$$\Gamma(\ell_\alpha \rightarrow \ell_\beta \gamma \phi) = \frac{\alpha m_\alpha}{64\pi^2} \left(|S_L^{\beta\alpha}|^2 + |S_R^{\beta\alpha}|^2 \right) \mathcal{I}(x_{\min}, y_{\min}), \tag{28}$$

where terms proportional to m_β/m_α have been neglected. Here $\mathcal{I}(x_{\min}, y_{\min})$ is a phase space integral given by

$$\mathcal{I}(x_{\min}, y_{\min}) = \int dx dy \frac{(x-1)(2-xy-y)}{y^2(1-x-y)}, \tag{29}$$

and we have introduced the usual dimensionless parameters x and y , defined as

$$x = \frac{2E_\beta}{m_\alpha}, \quad y = \frac{2E_\gamma}{m_\alpha}, \tag{30}$$

which, together with $z = 2E_\phi/m_\alpha$, must fulfill the kinematical condition $x + y + z = 2$. We point out that our analytical results match those in [53], except for redefinitions in the couplings.³

The phase space integral in Eq. (29) depends on x_{\min} and y_{\min} , the minimal values that the x and y parameters may take. While one could naively think that these are just dictated by kinematics, they are actually determined by the minimal ℓ_β lepton and photon energies measured in a given experiment. This not only properly adapts the calculation of the phase space integral to the physical region explored in a real experiment, but also cures the kinematical divergences that would otherwise appear. In fact, we note that the integral in Eq. (29) diverges when the photon energy vanishes ($y \rightarrow 0$). This is the well-known infrared divergence that also appears, for instance, in the radiative SM decay $\mu \rightarrow e\nu\bar{\nu}\gamma$. Another divergence is encountered when the photon and the ℓ_β lepton in the final state are emitted in the same direction. The angle between their momenta is given by

$$\cos\theta_{\beta\gamma} = 1 + \frac{2-2(x+y)}{xy}. \tag{31}$$

Since we work in the limit $m_\beta = 0$, one finds a colinear divergence in configurations in which the photon and the ℓ_β lepton have their momenta aligned ($\theta_{\beta\gamma} \rightarrow 0$). However, any real experimental setup has a finite experimental resolution, which implies a non-zero minimum

³In the model considered in [53], the right-handed coupling was suppressed and hence neglected.

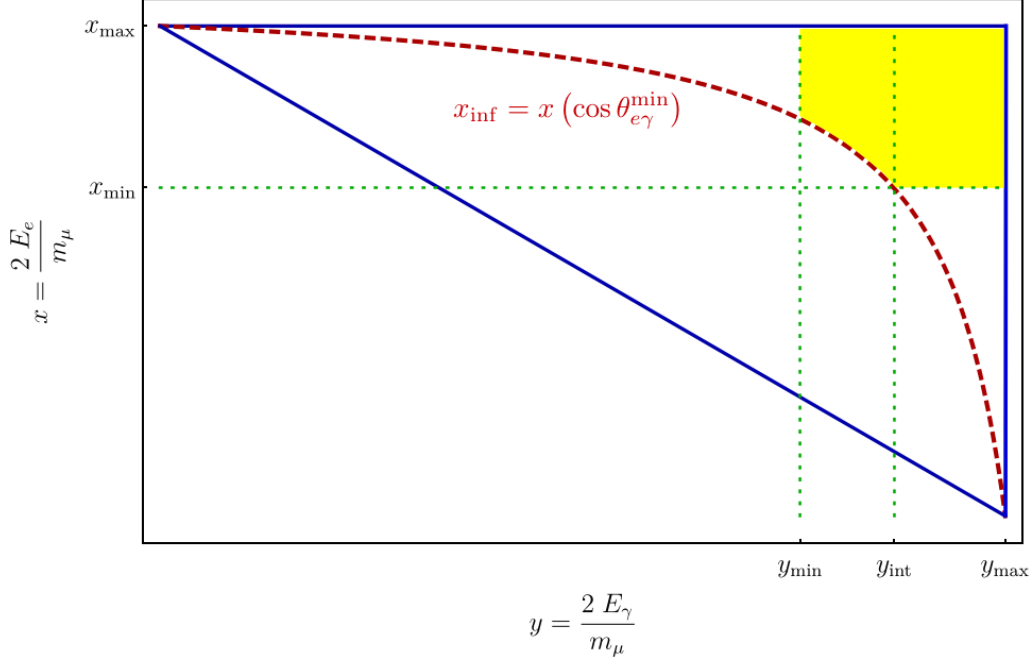


Figure 2: Illustration of the allowed phase space region for the process $\mu \rightarrow e \gamma \phi$ in a given experiment. The blue continuous lines correspond to $\cos \theta_{e\gamma} = \pm 1$ and therefore delimit the total phase space that would be in principle available due to kinematics. The red dashed line represents $x_{\text{inf}}(y)$ and corresponds to the minimal $\theta_{e\gamma}$ angle measurable by the experiment, excluding the region below it. The green dotted straight lines at x_{min} and y_{min} are the minimal positron and photon energy, respectively, that the experiment can measure, while y_{int} is the value of y for which x_{min} and x_{inf} intersect. Finally, the yellow surface is the region where we must integrate.

measurable E_γ and a non-zero minimum $\theta_{\beta\gamma}$ angle. Therefore, by restricting the phase space integration to the kinematical region explored in a practical situation, all divergences disappear.

Direct comparison with Eq. (22) allows one to establish the relation

$$\Gamma(\ell_\alpha \rightarrow \ell_\beta \gamma \phi) = \frac{\alpha}{2\pi} \mathcal{I}(x_{\text{min}}, y_{\text{min}}) \Gamma(\ell_\alpha \rightarrow \ell_\beta \phi), \quad (32)$$

which tells us that $\ell_\alpha \rightarrow \ell_\beta \gamma \phi$ is suppressed with respect to $\ell_\alpha \rightarrow \ell_\beta \phi$ due to an additional α coupling and a phase space factor. In fact, the latter turns out to be the main source of suppression.

In order to illustrate the calculation of the phase space integral for a specific case, let us focus on the $\mu \rightarrow e \gamma \phi$ decay and consider the MEG experiment [59]. This experiment has been designed to search for $\mu \rightarrow e \gamma$ and therefore concentrates on $E_e \simeq m_\mu/2$ and $\cos \theta_{e\gamma} \simeq -1$ (positron and photon emitted back to back). However, due to the finite experimental resolution, these cuts cannot be imposed with full precision, which makes MEG also sensitive to $\mu \rightarrow e \gamma \phi$. The final MEG results were obtained with the cuts [59]

$$\cos \theta_{e\gamma} < -0.99963 \quad , \quad 51.0 < E_\gamma < 55.5 \text{ MeV} \quad , \quad 52.4 < E_e < 55.0 \text{ MeV}. \quad (33)$$

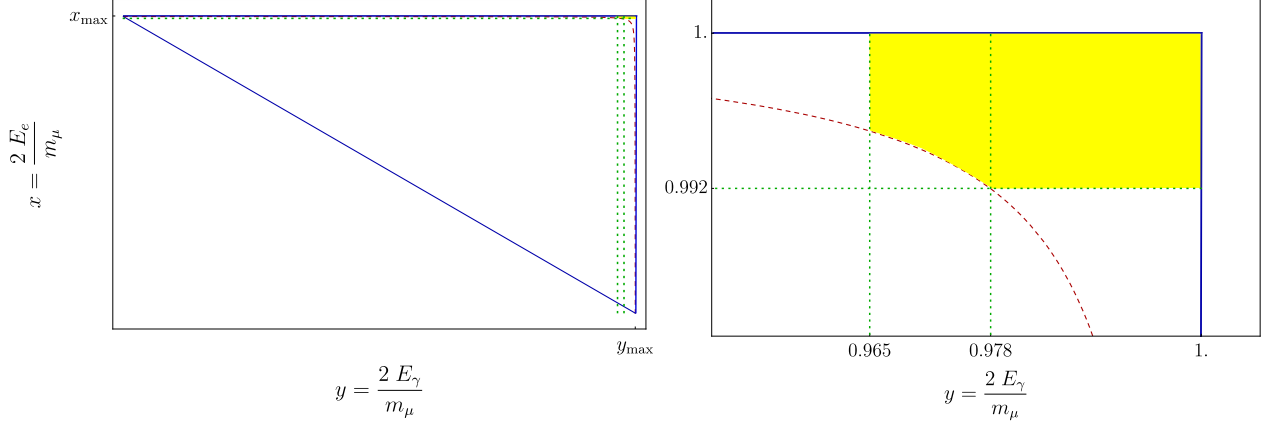


Figure 3: Realistic version of the phase space region limited by the experimental cuts of the MEG experiment, given in Eq. (33). The figure on the right shows a zoom of the figure on the left, centered on the colored surface.

This defines the MEG kinematical region for the calculation of the phase space integral in Eq. (29) since $\mu \rightarrow e \gamma \phi$ events that fall in this region can be detected by the experiment. For instance, events with $\cos \theta_{e\gamma} < -0.99963$, or equivalently $\theta_{e\gamma} > \theta_{e\gamma}^{\min} = 178.441^\circ$, were at the reach of MEG. The kinematical region can be divided into two subregions:

$$y_{\min} = \frac{2 E_{\gamma}^{\min}}{m_{\mu}} < y < y_{\text{int}}, \quad (34)$$

$$x_{\text{inf}} < x < x_{\max} = 1,$$

and

$$y_{\text{int}} < y < y_{\max} = 1,$$

$$x_{\min} = \frac{2 E_e^{\min}}{m_{\mu}} < x < x_{\max}, \quad (35)$$

where $x_{\text{inf}} = x_{\text{inf}}(y)$ is the value of x such that $\cos \theta_{e\gamma} = \cos \theta_{e\gamma}^{\min}$ for each value of y . This can be easily found by solving Eq. (31):

$$x_{\text{inf}} = \frac{2(1-y)}{2-y(1-\cos \theta_{e\gamma}^{\min})}. \quad (36)$$

Finally y_{int} is the value of y for which x_{\min} and x_{inf} coincide. These two subregions are illustrated in Fig. 2, where the experimental restrictions have been modified for the sake of clarity by enlarging the kinematical region of interest. A realistic representation obtained with the MEG cuts in Eq. (33) is shown in Fig. 3. This clearly illustrates the strong suppression due to the phase space integral.

Having explained how to compute the phase space integral and illustrated the strong suppression it introduces, we can obtain results for the MEG experiment. Using the cuts in Eq. (33), the phase space integral in Eq. (29) can be numerically computed to find

$$\mathcal{I}(x_{\min}, y_{\min})_{\text{MEG}} = 3.8 \times 10^{-8}. \quad (37)$$

| References | $\theta_{e\gamma}^{\min}$ | E_{γ}^{\min} [MeV] | E_e^{\min} [MeV] | $\mathcal{I}(x_{\min}, y_{\min})$ | BR bound | Limit on $ S^{e\mu} $ |
|------------|---------------------------|---------------------------|--------------------|-----------------------------------|-----------------------|-----------------------|
| [60] | 160° | 40 | 44 | 1.3×10^{-3} | 4.9×10^{-11} | 9.5×10^{-11} |
| [61, 62] | 140° | 38 | 38 | 1.1×10^{-2} | 1.1×10^{-9} | 1.6×10^{-10} |

Table 1: Results in the search for $\mu \rightarrow e\gamma\phi$ at the Crystal Box experiment.

Combining this result with Eq. (28), we obtain the branching ratio of $\mu \rightarrow e\gamma\phi$ restricted to the MEG phase space, obtaining

$$\text{BR}_{\text{MEG}}(\mu \rightarrow e\gamma\phi) = 1.5 \times 10^5 \left(|S_L^{e\mu}|^2 + |S_R^{e\mu}|^2 \right). \quad (38)$$

MEG results require $\text{BR}(\mu \rightarrow e\gamma) < 4.2 \times 10^{-13}$ [59], a bound that must also be satisfied by $\text{BR}_{\text{MEG}}(\mu \rightarrow e\gamma\phi)$. This leads to

$$|S^{e\mu}| < 1.6 \times 10^{-9}. \quad (39)$$

This bound is notably worse than the one given in Eq. (24), as expected due to the strong phase space suppression at MEG, an experiment that is clearly not designed to search for $\mu \rightarrow e\gamma\phi$.

More stringent bounds were obtained at the Crystal Box experiment at LAMPF [60–62]. Several searches were performed, with different experimental cuts and branching ratio bounds. These result in different limits on the $|S^{e\mu}|$ effective coupling, as shown in Table 1. Adapting the limit from the $\mu \rightarrow e\gamma$ search in [60] along the lines followed in the previous discussion for MEG, we find

$$|S^{e\mu}| < 9.5 \times 10^{-11}. \quad (40)$$

This bound is still not better than the one given in Eq. (24), but it is in the same ballpark. A very similar bound is obtained with the results of a later analysis, in this case more specific to $\mu \rightarrow e\gamma\phi$ [61, 62].

Finally, the Mu3e experiment is not well equipped to detect the photon in $\mu \rightarrow e\gamma\phi$ and therefore cannot improve on these limits. As explained in [56], a future *Mu3e-Gamma experiment* including a photon conversion layer could increase the sensitivity to $\mu \rightarrow e\gamma\phi$.

4.3 $\ell_{\alpha}^{-} \rightarrow \ell_{\beta}^{-} \ell_{\beta}^{-} \ell_{\beta}^{+}$

Complete expressions for the $\ell_{\alpha}^{-} \rightarrow \ell_{\beta}^{-} \ell_{\beta}^{-} \ell_{\beta}^{+}$ decay width in the absence of ϕ can be found in [63]. Here we are interested in the new contributions mediated by the scalar ϕ , which are given by the Feynman diagrams shown in Fig. 4. It is straightforward to derive the associated amplitude, given by

$$\begin{aligned} \mathcal{M}_{\phi} = & \bar{u}(p_3) i (S^{\beta\beta} P_L + S^{\beta\beta*} P_R) v(p_4) \frac{i}{q^2 + i\varepsilon} \bar{u}(p_2) i (S_L^{\beta\alpha} P_L + S_R^{\beta\alpha} P_R) u(p_1) \\ & - \bar{u}(p_2) i (S^{\beta\beta} P_L + S^{\beta\beta*} P_R) v(p_4) \frac{i}{k^2 + i\varepsilon} \bar{u}(p_3) i (S_L^{\beta\alpha} P_L + S_R^{\beta\alpha} P_R) u(p_1). \end{aligned} \quad (41)$$

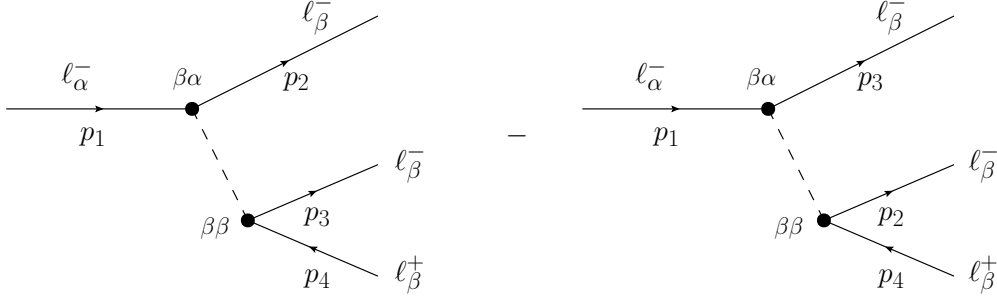


Figure 4: Tree-level Feynman diagrams contributing to the process $\ell_\alpha^- \rightarrow \ell_\beta^- \ell_\beta^- \ell_\beta^+$ described by the effective Lagrangian in Eq. (1).

Here u and v are spinors, $q = p_1 - p_2$ and $k = p_1 - p_3$ are the ϕ virtual momenta and we have explicitly indicated the flavor indices of the $S_{L,R}$ coefficients. Also, we define the diagonal couplings $S^{\beta\beta} \equiv S_L^{\beta\beta} + S_R^{\beta\beta*}$. The total decay width can then be written as

$$\Gamma(\ell_\alpha^- \rightarrow \ell_\beta^- \ell_\beta^- \ell_\beta^+) = \Gamma_{\bar{\phi}}(\ell_\alpha^- \rightarrow \ell_\beta^- \ell_\beta^- \ell_\beta^+) + \Gamma_\phi(\ell_\alpha^- \rightarrow \ell_\beta^- \ell_\beta^- \ell_\beta^+), \quad (42)$$

where $\Gamma_{\bar{\phi}}$ is the decay width in the absence of ϕ , given in [63], and

$$\begin{aligned} \Gamma_\phi(\ell_\alpha^- \rightarrow \ell_\beta^- \ell_\beta^- \ell_\beta^+) = & \\ & \frac{m_\alpha}{512\pi^3} \left\{ \left(|S_L^{\beta\alpha}|^2 + |S_R^{\beta\alpha}|^2 \right) \left\{ |S^{\beta\beta}|^2 \left(4 \log \frac{m_\alpha}{m_\beta} - \frac{49}{6} \right) - \frac{2}{6} \left[(S^{\beta\beta*})^2 + (S^{\beta\beta})^2 \right] \right\} \right. \\ & - \frac{m_\alpha^2}{6} \left[S_L^{\beta\alpha} S^{\beta\beta} A_{LL}^{S*} + 2S_L^{\beta\alpha} S^{\beta\beta*} A_{LR}^{S*} + 2S_R^{\beta\alpha} S^{\beta\beta} A_{RL}^{S*} + S_R^{\beta\alpha} S^{\beta\beta*} A_{RR}^{S*} \right. \\ & - 12 \left(S_L^{\beta\alpha} S^{\beta\beta} A_{LL}^{T*} + S_R^{\beta\alpha} S^{\beta\beta*} A_{RR}^{T*} \right) - 4 \left(S_R^{\beta\alpha} S^{\beta\beta} A_{RL}^{V*} + S_L^{\beta\alpha} S^{\beta\beta*} A_{LR}^{V*} \right) \\ & \left. \left. + 6e^2 \left(S_R^{\beta\alpha} S^{\beta\beta} K_2^{L*} + S_L^{\beta\alpha} S^{\beta\beta*} K_2^{R*} \right) + \text{c.c.} \right] \right\}. \end{aligned} \quad (43)$$

In writing Eq. (43) we have only kept the lowest order terms in powers of m_β for each possible combination of couplings. This is equivalent to 0th order for all terms, with the exception of the ones in the first line, where the factor $\log \frac{m_\alpha}{m_\beta}$ avoids the appearance of an infrared divergence. An expression including terms up to first order in m_β is given in Sec. A.

In order to evaluate the relevance of the new contributions mediated by the scalar ϕ we drop the 4-fermion operators in Eq. (4) and consider a simplified effective Lagrangian containing only left-handed photonic dipole and scalar-mediated operators

$$\mathcal{L}_{\text{LFV}}^{\text{simp}} = \frac{e m_\alpha K_2^L}{2} \bar{\ell}_\beta \sigma^{\mu\nu} P_L \ell_\alpha F_{\mu\nu} + S_L \phi \bar{\ell}_\beta P_L \ell_\alpha + \text{h.c.} \quad (44)$$

Then, inspired by [64], we parametrize the K_2^L and S_L coefficients as

$$e K_2^L \equiv \frac{1}{(\kappa + 1) \Lambda^2}, \quad S_L \equiv m_\alpha \frac{\kappa}{(\kappa + 1) \Lambda}. \quad (45)$$

Λ is a dimensionful parameter that represents the energy scale at which these coefficients are induced, while κ is a dimensionless parameter that accounts for the relative intensity of

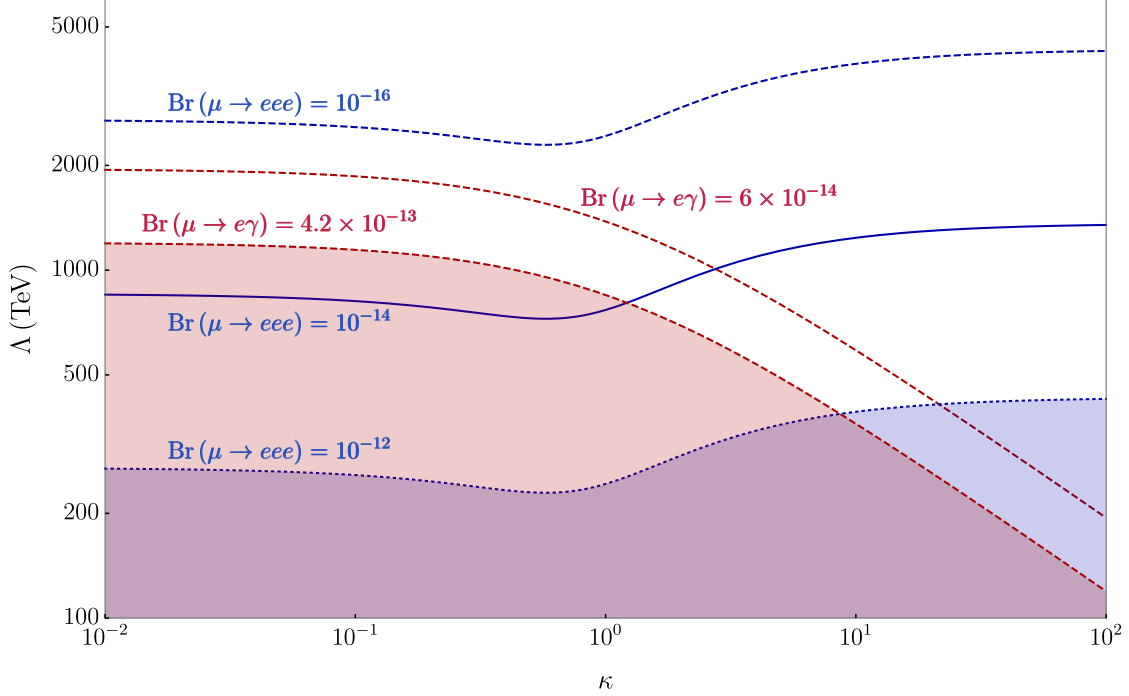


Figure 5: Contours of $\text{BR}(\mu \rightarrow e\gamma)$ and $\text{BR}(\mu \rightarrow eee)$ in the κ - Λ plane. The lowest values correspond to the future sensitivities for the MEG-II and Mu3e experiments, while colored regions are excluded due to the current bounds $\text{BR}(\mu \rightarrow e\gamma) < 4.2 \cdot 10^{-13}$ and $\text{BR}(\mu \rightarrow eee) < 10^{-12}$. These results have been obtained with the effective Lagrangian in Eq. (1) and the parametrization in Eq. (45).

these two interactions. In case of $\kappa \ll 1$, the dipole operator dominates, while the scalar mediated contribution dominates for $\kappa \gg 1$. We point out that m_α in Eqs. (44) and (45) is a global factor given by the mass of the heaviest charged lepton in the process and that Eq. (45) assumes $S_L^{\beta\alpha} = S_L^{\beta\beta}$.

Fig. 5 shows $\text{BR}(\mu \rightarrow e\gamma)$ and $\text{BR}(\mu \rightarrow eee)$ as a function of Λ and κ . Our results are compared to the current bounds and the future sensitivities for the MEG-II and Mu3e experiments. We observe that for $\kappa \gg 1$ and $\text{BR}(\mu \rightarrow eee) > 10^{-16}$, Λ must be necessarily below ~ 3000 TeV. A slightly lower upper limit for Λ is found when $\kappa \ll 1$ and $\text{BR}(\mu \rightarrow e\gamma) > 10^{-14}$. These are precisely the final expected sensitivities in MEG-II and Mu3e. Furthermore, we note that the search for the scalar mediated contribution in Mu3e will actually be very constraining in all the parameter space.

4.4 $\ell_\alpha^- \rightarrow \ell_\beta^- \ell_\gamma^- \ell_\gamma^+$

Again, complete expressions for the $\ell_\alpha^- \rightarrow \ell_\beta^- \ell_\gamma^- \ell_\gamma^+$ decay width in the absence of ϕ can be found in [63]. The new contributions mediated by the scalar ϕ are obtained from the Feynman diagrams shown in Fig. 6. While the diagram on the left involves a flavor conserving ($\gamma\gamma$) and a flavor violating ($\beta\alpha$) vertex, both vertices in the diagram on the right violate flavor ($\gamma\alpha$ and $\gamma\beta$). The associated amplitude is slightly different from that of the previous process

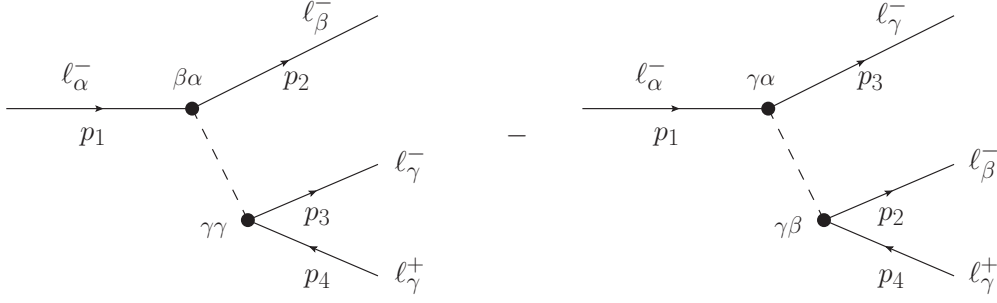


Figure 6: Tree-level Feynman diagrams contributing to the process $\ell_\alpha^- \rightarrow \ell_\beta^- \ell_\gamma^- \ell_\gamma^+$ described by the effective Lagrangian in Eq. (1).

and is given by

$$\begin{aligned} \mathcal{M}_\phi = & \bar{u}(p_3) i (S^{\gamma\gamma} P_L + S^{\gamma\gamma*} P_R) v(p_4) \frac{i}{q^2 + i\varepsilon} \bar{u}(p_2) i \left(S_L^{\beta\alpha} P_L + S_R^{\beta\alpha} P_R \right) u(p_1) \\ & - \bar{u}(p_2) i \left(S_L^{\gamma\beta} P_L + S_R^{\gamma\beta} P_R \right) v(p_4) \frac{i}{k^2 + i\varepsilon} \bar{u}(p_3) i \left(S_L^{\gamma\alpha} P_L + S_R^{\gamma\alpha} P_R \right) u(p_1). \end{aligned} \quad (46)$$

Finally, the total decay width can be written as

$$\Gamma(\ell_\alpha^- \rightarrow \ell_\beta^- \ell_\gamma^- \ell_\gamma^+) = \Gamma_{\bar{\phi}}(\ell_\alpha^- \rightarrow \ell_\beta^- \ell_\gamma^- \ell_\gamma^+) + \Gamma_\phi(\ell_\alpha^- \rightarrow \ell_\beta^- \ell_\gamma^- \ell_\gamma^+), \quad (47)$$

where $\Gamma_{\bar{\phi}}$ is the decay width in the absence of ϕ , given in [63], and

$$\begin{aligned} \Gamma_\phi(\ell_\alpha^- \rightarrow \ell_\beta^- \ell_\gamma^- \ell_\gamma^+) = & \frac{m_\alpha}{512\pi^3} \left\{ \left(|S_L^{\beta\alpha}|^2 + |S_R^{\beta\alpha}|^2 \right) \left\{ |S^{\gamma\gamma}|^2 \left(4 \log \frac{m_\alpha}{m_\gamma} - \frac{23}{3} \right) - \frac{1}{3} [(S^{\gamma\gamma*})^2 + (S^{\gamma\gamma})^2] \right\} \right. \\ & + \left(|S_L^{\gamma\alpha}|^2 + |S_R^{\gamma\alpha}|^2 \right) \left(|S_L^{\gamma\beta}|^2 + |S_R^{\gamma\beta}|^2 \right) \left(2 \log \frac{m_\alpha}{m_f^{\max}} - 3 \right) \\ & - \frac{1}{2} \left[S^{\gamma\gamma} \left(S_L^{\beta\alpha} S_L^{\gamma\alpha*} S_L^{\gamma\beta*} + S_R^{\beta\alpha*} S_R^{\gamma\alpha} S_R^{\gamma\beta} \right) + \text{c.c.} \right] \\ & + \frac{m_\alpha^2}{6} \left[S_L^{\gamma\alpha} S_L^{\gamma\beta} A_{LL}^{S*} + S_R^{\gamma\alpha} S_R^{\gamma\beta} A_{RR}^{S*} - 2 S^{\gamma\gamma} \left(S_L^{\beta\alpha} A_{LL}^{S*} + S_L^{\beta\alpha*} A_{LR}^S + S_R^{\beta\alpha} A_{RL}^{S*} + S_R^{\beta\alpha*} A_{RR}^S \right) \right. \\ & + 4 \left(S_L^{\gamma\alpha} S_R^{\gamma\beta} A_{LR}^{V*} + S_R^{\gamma\alpha} S_L^{\gamma\beta} A_{RL}^{V*} \right) + 12 \left(S_L^{\gamma\alpha} S_L^{\gamma\beta} A_{LL}^{T*} + S_R^{\gamma\alpha} S_R^{\gamma\beta} A_{RR}^{T*} \right) \\ & \left. - 6e^2 \left(S_L^{\gamma\alpha} S_R^{\gamma\beta} K_2^{R*} + S_R^{\gamma\alpha} S_L^{\gamma\beta} K_2^{L*} \right) + \text{c.c.} \right\}. \end{aligned} \quad (48)$$

Here $m_f^{\max} = \max(m_\beta, m_\gamma)$ and then the expression depends on the process in question. Once again, we have only kept the lowest order terms in powers of m_β and m_γ for each possible combination of couplings.

4.5 $\ell_\alpha^- \rightarrow \ell_\beta^+ \ell_\gamma^- \ell_\gamma^-$

Also for this process, complete expressions for the $\ell_\alpha^- \rightarrow \ell_\beta^+ \ell_\gamma^- \ell_\gamma^-$ decay width in the absence of ϕ can be found in [63]. The new contributions mediated by the scalar ϕ are given by

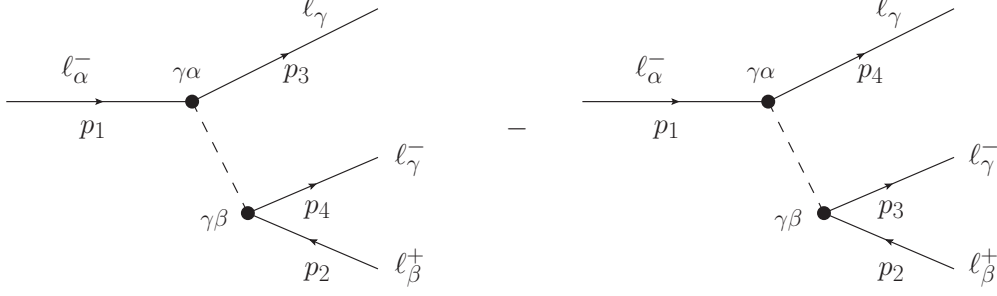


Figure 7: Tree-level Feynman diagrams contributing to the process $\ell_\alpha^- \rightarrow \ell_\beta^+ \ell_\gamma^- \ell_\gamma^-$ described by the effective Lagrangian in Eq. (1).

the Feynman diagrams shown in Fig. 7. We note that both vertices are necessarily flavor violating. The associated amplitude is given in this case by

$$\begin{aligned} \mathcal{M}_\phi &= \bar{u}(p_4) i \left(S_L^{\gamma\beta} P_L + S_R^{\gamma\beta} P_R \right) v(p_2) \frac{i}{q^2 + i\varepsilon} \bar{u}(p_3) i \left(S_L^{\gamma\alpha} P_L + S_R^{\gamma\alpha} P_R \right) u(p_1) \\ &\quad - \bar{u}(p_3) i \left(S_L^{\gamma\beta} P_L + S_R^{\gamma\beta} P_R \right) v(p_2) \frac{i}{k^2 + i\varepsilon} \bar{u}(p_4) i \left(S_L^{\gamma\alpha} P_L + S_R^{\gamma\alpha} P_R \right) u(p_1). \end{aligned} \quad (49)$$

Here $q = p_1 - p_3$ and $k = p_1 - p_4$ are different from their definitions in the processes above. Writing one more time the decay width as the sum of two contributions,

$$\Gamma(\ell_\alpha^- \rightarrow \ell_\beta^+ \ell_\gamma^- \ell_\gamma^-) = \Gamma_{\bar{\phi}}(\ell_\alpha^- \rightarrow \ell_\beta^+ \ell_\gamma^- \ell_\gamma^-) + \Gamma_\phi(\ell_\alpha^- \rightarrow \ell_\beta^+ \ell_\gamma^- \ell_\gamma^-), \quad (50)$$

where $\Gamma_{\bar{\phi}}$ is the decay width in the absence of ϕ , given in [63], we find that

$$\begin{aligned} \Gamma_\phi(\ell_\alpha^- \rightarrow \ell_\beta^+ \ell_\gamma^- \ell_\gamma^-) &= \\ &\frac{m_\alpha}{512\pi^3} \left\{ \left(|S_L^{\gamma\alpha}|^2 + |S_R^{\gamma\alpha}|^2 \right) \left(|S_L^{\gamma\beta}|^2 + |S_R^{\gamma\beta}|^2 \right) \left(2 \log \frac{m_\alpha}{m_f^{\max}} - 3 \right) \right. \\ &\quad - \frac{1}{2} \left(|S_L^{\gamma\alpha}|^2 |S_L^{\gamma\beta}|^2 + |S_R^{\gamma\alpha}|^2 |S_R^{\gamma\beta}|^2 \right) \\ &\quad + \frac{m_\alpha^2}{6} \left[-S_L^{\gamma\alpha} S_L^{\gamma\beta} A_{LL}^{S*} - S_R^{\gamma\alpha} S_R^{\gamma\beta} A_{RR}^{S*} - 2 \left(S_L^{\gamma\alpha} S_R^{\gamma\beta} A_{RL}^{S*} + S_R^{\gamma\alpha} S_L^{\gamma\beta} A_{LR}^{S*} \right) \right. \\ &\quad \left. \left. + 4 \left(S_L^{\gamma\alpha} S_R^{\gamma\beta} A_{RL}^{V*} + S_R^{\gamma\alpha} S_L^{\gamma\beta} A_{LR}^{V*} \right) + 12 \left(S_L^{\gamma\alpha} S_L^{\gamma\beta} A_{LL}^{T*} + S_R^{\gamma\alpha} S_R^{\gamma\beta} A_{RR}^{T*} \right) + \text{c.c.} \right] \right\}, \end{aligned} \quad (51)$$

where $m_f^{\max} = \max(m_\beta, m_\gamma)$.

4.6 Lepton anomalous magnetic moments

At present, there is a discrepancy between the experimental determination of the electron and muon anomalous magnetic moments and their SM predicted values [65–71]

$$\Delta a_e = a_e^{\text{exp}} - a_e^{\text{SM}} = (-87 \pm 36) \times 10^{-14}, \quad (52)$$

$$\Delta a_\mu = a_\mu^{\text{exp}} - a_\mu^{\text{SM}} = (27.1 \pm 7.3) \times 10^{-10}, \quad (53)$$

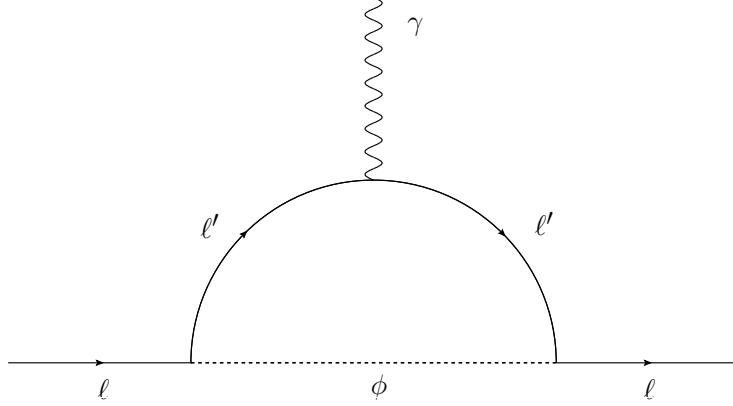


Figure 8: Feynman diagram for the one-loop contribution to the anomalous magnetic moment of charged leptons given by the interaction in Eq. (1).

where

$$a_\beta = \frac{g_\beta - 2}{2}. \quad (54)$$

In the case of the muon anomalous magnetic moment, the deviation is at the level of $\sim 4\sigma$, whereas for the electron anomalous magnetic moment the significance is a little lower, slightly below $\sim 3\sigma$. While further measurements (and possibly improved theoretical calculations) are required to fully confirm these anomalies, these intriguing deviations can be interpreted as a possible hint of new physics [72].

The charged leptons anomalous magnetic moments also receive contributions mediated by the scalar ϕ . We show in Fig. 8 the relevant Feynman diagram. We will assume that the dominant contribution is induced by lepton flavor conserving (diagonal) couplings, and therefore take $\ell' = \ell$. We find the simple expression

$$\Delta a_\beta = \frac{1}{16\pi^2} \left[3 (\text{Re } S^{\beta\beta})^2 - (\text{Im } S^{\beta\beta})^2 \right], \quad (55)$$

which agrees with previous results in the literature. In particular, it matches exactly the expression given in [73] in the limit of a massless scalar, with the equivalence

$$-\frac{m_\beta}{v} a_\beta^S = \frac{1}{2} (S^{\beta\beta} + S^{\beta\beta*}), \quad -i \frac{m_\beta}{v} b_\beta^S = -\frac{1}{2} (S^{\beta\beta} - S^{\beta\beta*}). \quad (56)$$

Now we are able to compare with the experimental measurements. Figure 9 shows favored regions for the diagonal coupling $S^{\beta\beta}$, with $\beta = e, \mu$, due to the electron and muon anomalous magnetic moments. Results for S^{ee} derived from $(g-2)_e$ measurements are shown on the left panel, whereas the right panel shows results for $S^{\mu\mu}$ as obtained from $(g-2)_\mu$ measurements. Given the low significance of the $(g-2)_e$ anomaly, one stays within the 3σ region even if $S^{ee} = 0$, but a value of about $|S^{ee}| \sim 10^{-5}$ is required in order to achieve agreement at the 1σ level. The deviation in $(g-2)_\mu$ is more significant, and this implies that one must introduce larger $S^{\mu\mu}$ values in order to reconcile the theoretical prediction with the experimental measurement. In this case, $S^{\mu\mu}$ couplings of the order of 10^{-4} are necessary. In both cases, the required values are in conflict with the bounds discussed in Sec. 3, see

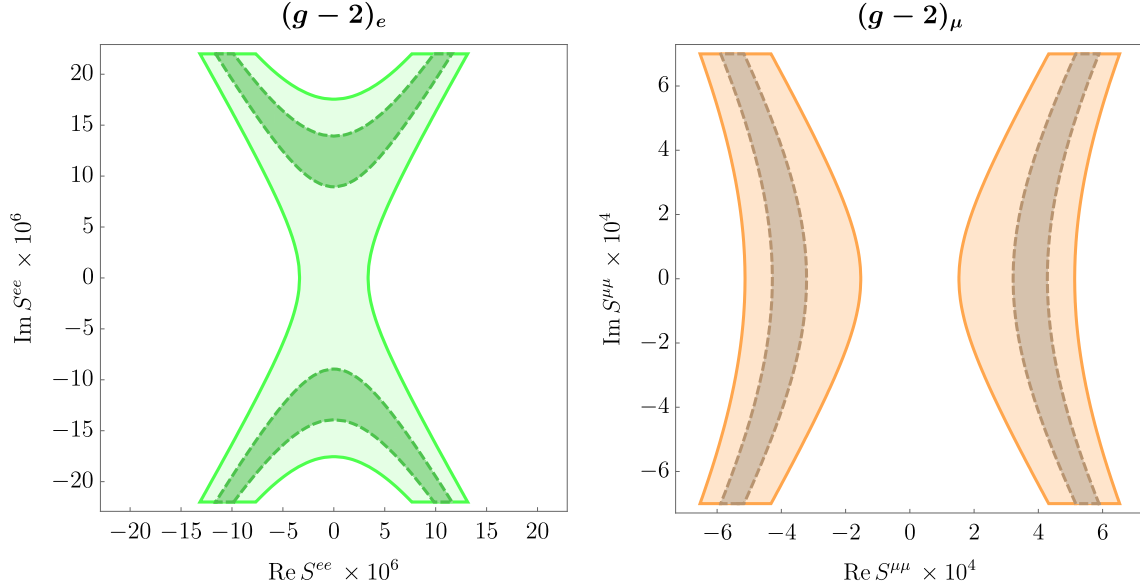


Figure 9: Favored regions for the diagonal coupling $S^{\beta\beta}$, with $\beta = e, \mu$, due to the electron (left) and muon (right) anomalous magnetic moments. Within the light (dark) region, the deviations in the charged lepton anomalous magnetic moments are explained at the 3σ (1σ) level.

Eqs. (7) and (8), and therefore a mechanism to suppress the processes from which they are derived would be necessary for the ultralight scalar ϕ to be able to provide an explanation to the current $g - 2$ anomalies.

5 Conclusions

Ultralight scalars appear in a wide variety of SM extensions, either as very light states or as exactly massless Goldstone bosons. Examples include the axion and the majoron, two well-motivated hypothetical particles at the core of two fundamental problems: the conservation of CP in the strong interactions and the origin of neutrino masses. These states, as well as other ultralight scalars, can be produced in many leptonic processes or act as their mediators, leading to many exotic signatures.

In this work we have explored the impact of ultralight scalars in many leptonic observables. We have adopted a model independent general approach, taking into account both scalar and pseudoscalar interactions to charged leptons, therefore going beyond most existing studies. First, we have briefly reviewed the current bounds from stellar cooling, which set important constraints on the diagonal couplings, and discussed indirect limits from the 1-loop generation of a coupling to photons. Then, we have revisited the decays $l_\alpha \rightarrow l_\beta \phi$ and $l_\alpha \rightarrow l_\beta \gamma \phi$, in which the scalar ϕ is produced, and provided complete expressions for the LFV 3-body decays $l_\alpha^- \rightarrow l_\beta^- l_\beta^- l_\beta^+$, $l_\alpha^- \rightarrow l_\beta^- l_\gamma^- l_\gamma^+$ and $l_\alpha^- \rightarrow l_\beta^+ l_\gamma^- l_\gamma^-$, in which ϕ contributes as mediator. Finally, the effect of ultralight scalars on the charged leptons anomalous magnetic moments has also been discussed.

The phenomenology of ultralight scalars is very rich, since they are kinematically accessible in most high- and low-energy processes. We have discussed many purely leptonic processes, but if ϕ couples to quarks as well, many hadronic and semi-leptonic channels open. This could give rise to many signatures at kaon factories [74]. Furthermore, ultralight scalars may leave their footprints in other processes. For instance, they can be produced and emitted in tritium beta decay [75] or $\mu - e$ conversion in nuclei [76], have a strong impact in leptogenesis [77], and give rise to non-resonant phenomena at colliders [78]. In our opinion, this diversity of experimental signatures and their potential to unravel some of the most important problems in particle physics through their connection to ultralight scalars merits further investigation.

Acknowledgements

The authors are grateful to Julian Heeck, Mario Reig and Martin Hirsch for fruitful discussions. Work supported by the Spanish grants FPA2017-85216-P (MINECO/AEI/FEDER, UE), SEJI/2018/033 (Generalitat Valenciana) and FPA2017-90566-REDC (Red Consolider MultiDark). The work of PE is supported by the FPI grant PRE2018-084599. AV acknowledges financial support from MINECO through the Ramón y Cajal contract RYC2018-025795-I.

A Parametrization in terms of derivative interactions

Eq. (1) is completely general and includes both scalar and pseudoscalar interactions of the field ϕ with a pair of charged leptons. An alternative parametrization in terms of derivative interactions is given by

$$\mathcal{L}_{\ell\ell\phi} = (\partial_\mu\phi) \bar{\ell}_\beta\gamma^\mu \left(\tilde{S}_L P_L + \tilde{S}_R P_R \right) \ell_\alpha + \text{h.c.} . \quad (57)$$

The coefficients $\tilde{S}_{L,R}$ have dimensions of mass^{-1} and carry flavor indices, omitted for the sake of clarity. Notice that the diagonal $\ell_\beta - \ell_\beta - \phi$ vertex is proportional to $(\tilde{S}_L + \tilde{S}_L^*)^{\beta\beta} P_L + (\tilde{S}_R + \tilde{S}_R^*)^{\beta\beta} P_R$, and therefore the diagonal couplings can be taken to be real without loss of generality. As will be shown below, Eq. (57) only includes pseudoscalar interactions for ϕ . Therefore, it can be thought of as a particularization of Eq. (1).⁴

Physical observables must be independent of the parametrization chosen. We proceed to show now that the two parametrizations considered here are completely equivalent for a pure pseudoscalar in processes involving on-shell leptons. First, we recall the equations of

⁴The parametrization in Eq. (57) is completely general if ϕ is a pure pseudoscalar, usually the case of the Goldstone bosons in many models. In such scenarios, the two parametrizations for the effective Lagrangian $\mathcal{L}_{\ell\ell\phi}$ introduced here are related to two possible ways to parametrize the Goldstone boson. Eq. (1) follows from a *cartesian parametrization*, that splits a complex scalar field in terms of its real and imaginary components. Alternatively, the parametrization in terms of derivative interactions in Eq. (57) would follow from a *polar parametrization*, that splits a complex scalar field in terms of its modulus and phase. As we will prove below, they lead to the same results for observables involving on-shell leptons.

motion for the lepton fields ℓ_α and its conjugate $\bar{\ell}_\alpha$

$$\begin{aligned} i \gamma^\mu \partial_\mu \ell_\alpha - m_\alpha \ell_\alpha &= 0, \\ i \partial_\mu \bar{\ell}_\alpha \gamma^\mu + m_\alpha \bar{\ell}_\alpha &= 0, \end{aligned} \quad (58)$$

valid for on-shell leptons. One can now rewrite Eq. (57) as the sum of a total derivative and a derivative acting on the lepton fields. The total derivative does not contribute to the action, whereas the derivative on the lepton fields can be replaced using the equations of motion in Eq. (58). This leads to

$$\begin{aligned} \mathcal{L}_{\ell\ell\phi} &= -i \phi \bar{\ell}_\beta \left[\left(m_\beta \tilde{S}_L^{\beta\alpha} - m_\alpha \tilde{S}_R^{\beta\alpha} \right) P_L + \left(m_\beta \tilde{S}_R^{\beta\alpha} - m_\alpha \tilde{S}_L^{\beta\alpha} \right) P_R \right] \ell_\alpha + \text{h.c.} \\ &\equiv \phi \bar{\ell}_\beta \left(S_L^{\beta\alpha} P_L + S_R^{\beta\alpha} P_R \right) \ell_\alpha + \text{h.c.} . \end{aligned} \quad (59)$$

Therefore we find a *dictionary* between the S_X and \tilde{S}_X coefficients

$$S_L^{\beta\alpha} = i \left(m_\alpha \tilde{S}_R^{\beta\alpha} - m_\beta \tilde{S}_L^{\beta\alpha} \right), \quad (60)$$

$$S_R^{\beta\alpha} = i \left(m_\alpha \tilde{S}_L^{\beta\alpha} - m_\beta \tilde{S}_R^{\beta\alpha} \right), \quad (61)$$

which for the diagonal couplings reduces to

$$S^{\beta\beta} = S_L^{\beta\beta} + (S_R^*)^{\beta\beta} = 2i m_\beta \left(\tilde{S}_R^{\beta\beta} - \tilde{S}_L^{\beta\beta} \right). \quad (62)$$

Since both $\tilde{S}_X^{\beta\beta}$ are real parameters, Eq. (62) implies that the diagonal $S^{\beta\beta}$ couplings must be purely imaginary. It is straightforward to show that, in this case, the flavor conserving interactions of ϕ in Eq. (1) are proportional to γ_5 (see Eq. (6)). This proves that Eq. (57) is not general, but only includes pseudoscalar interactions, and there is no one-to-one correspondence between the two parametrizations. Given a set of \tilde{S}_X couplings, one can always find the corresponding S_X couplings using Eqs. (60) and (61). However, certain sets of S_X couplings, namely those with non-vanishing real parts, cannot be expressed in terms of \tilde{S}_X couplings. This stems from the fact that purely scalar interactions are not included in Eq. (57).

The equivalence for the case of a pure pseudoscalar can be explicitly illustrated by comparing the analytical expressions obtained with Eqs. (1) and (57) for a given observable. We can start with a trivial example, the process $\ell_\alpha \rightarrow \ell_\beta \phi$, discussed in Sec. 4.1. Using the parametrization in Eq. (57), one can easily derive the decay width of this two-body decay,

$$\tilde{\Gamma}(\ell_\alpha \rightarrow \ell_\beta \phi) = \frac{m_\alpha^3}{32\pi} \left(\left| \tilde{S}_L^{\beta\alpha} \right|^2 + \left| \tilde{S}_R^{\beta\alpha} \right|^2 \right), \quad (63)$$

where terms proportional to m_β have been neglected. This results differs from Eq. (22) only by a factor m_α^2 , as one would obtain from the direct application of the dictionary in Eqs. (60) and (61). Let us now consider a less trivial example: $\ell_\alpha^- \rightarrow \ell_\beta^- \ell_\beta^+ \ell_\beta^-$. The computation of its

amplitude with the Lagrangian in Eq. (57) makes use of the same Feynman diagrams shown in Fig. 4. In this case one obtains

$$\begin{aligned} \widetilde{\mathcal{M}}_\phi &= \bar{u}(p_3) 2(-\not{q}) \left(\widetilde{S}_L^{\beta\beta} P_L + \widetilde{S}_R^{\beta\beta} P_R \right) v(p_4) \frac{i}{q^2 + i\varepsilon} \bar{u}(p_2) (\not{q}) \left(\widetilde{S}_L^{\beta\alpha} P_L + \widetilde{S}_R^{\beta\alpha} P_R \right) u(p_1) \\ &\quad - \bar{u}(p_2) 2(-\not{k}) \left(\widetilde{S}_L^{\beta\beta} P_L + \widetilde{S}_R^{\beta\beta} P_R \right) v(p_4) \frac{i}{k^2 + i\varepsilon} \bar{u}(p_3) (\not{k}) \left(\widetilde{S}_L^{\beta\alpha} P_L + \widetilde{S}_R^{\beta\alpha} P_R \right) u(p_1), \end{aligned} \quad (64)$$

where the factor of 2 preceding the diagonal coupling is due to the addition of the Hermitian conjugate, as explicitly shown in Eq. (57). Again, explicit flavor indices have been introduced. The decay width is computed to be

$$\begin{aligned} \widetilde{\Gamma}_\phi(\ell_\alpha^- \rightarrow \ell_\beta^- \ell_\beta^+ \ell_\beta^-) &= \\ &\frac{m_\alpha^5}{512\pi^3} \left\{ 4 \left(|\widetilde{S}_L^{\beta\alpha}|^2 + |\widetilde{S}_R^{\beta\alpha}|^2 \right) \left(\widetilde{S}_L^{\beta\beta} - \widetilde{S}_R^{\beta\beta} \right)^2 \frac{m_\beta^2}{m_\alpha^2} \left(4 \log \frac{m_\alpha}{m_\beta} - \frac{15}{2} \right) \right. \\ &\quad + \frac{m_\beta}{3m_\alpha} \left\{ \left(\widetilde{S}_L^{\beta\beta} - \widetilde{S}_R^{\beta\beta} \right) \left\{ \widetilde{S}_R^{\beta\alpha} (A_{LL}^{S*} - 2A_{LR}^{S*}) - \widetilde{S}_L^{\beta\alpha} (A_{RR}^{S*} - 2A_{RL}^{S*}) \right. \right. \\ &\quad \left. \left. + \frac{m_\beta}{m_\alpha} \left\{ \widetilde{S}_L^{\beta\alpha} \left[2A_{LL}^{S*} + \left(12 \log \frac{m_\alpha}{m_\beta} - 25 \right) A_{LR}^{S*} \right] - \widetilde{S}_R^{\beta\alpha} \left[2A_{RR}^{S*} + \left(12 \log \frac{m_\alpha}{m_\beta} - 25 \right) A_{RL}^{S*} \right] \right\} \right. \\ &\quad \left. + 12 \left[A_{RR}^{T*} \left(\widetilde{S}_L^{\beta\alpha} + 2 \frac{m_\beta}{m_\alpha} \widetilde{S}_R^{\beta\alpha} \right) - A_{LL}^{T*} \left(\widetilde{S}_R^{\beta\alpha} + 2 \frac{m_\beta}{m_\alpha} \widetilde{S}_L^{\beta\alpha} \right) \right] + 4 \left(\widetilde{S}_R^{\beta\alpha} A_{LR}^{V*} - \widetilde{S}_L^{\beta\alpha} A_{RL}^{V*} \right) \right. \\ &\quad \left. + 2 \frac{m_\beta}{m_\alpha} \left\{ \widetilde{S}_L^{\beta\alpha} \left[\left(25 - 12 \log \frac{m_\alpha}{m_\beta} \right) A_{LR}^{V*} - \left(42 - 24 \log \frac{m_\alpha}{m_\beta} \right) A_{LL}^{V*} \right] \right. \right. \\ &\quad \left. \left. - \widetilde{S}_R^{\beta\alpha} \left[\left(25 - 12 \log \frac{m_\alpha}{m_\beta} \right) A_{RL}^{V*} - \left(42 - 24 \log \frac{m_\alpha}{m_\beta} \right) A_{RR}^{V*} \right] \right\} + 6e^2 \left[K_2^{L*} \widetilde{S}_L^{\beta\alpha} - K_2^{R*} \widetilde{S}_R^{\beta\alpha} \right] \right. \\ &\quad \left. + 4e^2 \frac{m_\beta}{m_\alpha} \left(\frac{3}{2} + \pi^2 + 6 \log^2 2 - 6 \log^2 \frac{m_\alpha}{m_\beta} \right) \left(K_2^{R*} \widetilde{S}_L^{\beta\alpha} - K_2^{L*} \widetilde{S}_R^{\beta\alpha} \right) \right\} + \text{c.c.} \left. \right\}. \end{aligned} \quad (65)$$

We note that infrared divergences also occur in interference terms at this order in $\frac{m_\beta}{m_\alpha}$. This explains the appearance of several log factors. The decay width in Eq. (65) can be compared to a previous result in the literature. The authors of [27] drop all interference terms in their calculation, and then their result must be compared to the first line in Eq. (65). One can easily relate the $\widetilde{S}_{L,R}$ coefficients to the ones in [27] as

$$V_{\beta\alpha}^e \equiv -\frac{1}{2} \left(\widetilde{S}_L^{\beta\alpha} + \widetilde{S}_R^{\beta\alpha} \right), \quad A_{\beta\alpha}^e \equiv \frac{1}{2} \left(\widetilde{S}_R^{\beta\alpha} - \widetilde{S}_L^{\beta\alpha} \right), \quad (66)$$

for the flavor violating terms, and

$$A_{\beta\beta}^e \equiv \left(\widetilde{S}_R^{\beta\beta} - \widetilde{S}_L^{\beta\beta} \right), \quad (67)$$

for the flavor conserving ones. With this translation, it is easy to check that both results agree up to a global factor of 1/2.

In order to compare the $\ell_\alpha^- \rightarrow \ell_\beta^- \ell_\beta^+ \ell_\beta^-$ decay widths obtained with both parametrizations we need an expanded version of Eq. (43) that includes terms up to $\mathcal{O}\left(\frac{m_\beta}{m_\alpha}\right)$. This is given by

$$\begin{aligned}
\Gamma_\phi(\ell_\alpha^- \rightarrow \ell_\beta^- \ell_\beta^+ \ell_\beta^-) = & \\
& \frac{m_\alpha}{512\pi^3} \left\{ \left(|S_L^{\beta\alpha}|^2 + |S_R^{\beta\alpha}|^2 \right) \left\{ |S^{\beta\beta}|^2 \left(4 \log \frac{m_\alpha}{m_\beta} - \frac{49}{6} \right) - \frac{2}{6} \left[(S^{\beta\beta*})^2 + (S^{\beta\beta})^2 \right] \right\} \right. \\
& - \frac{m_\alpha^2}{6} \left\{ S_L^{\beta\alpha} S^{\beta\beta} A_{LL}^{S*} + 2S_L^{\beta\alpha} S^{\beta\beta*} A_{LR}^{S*} + 2S_R^{\beta\alpha} S^{\beta\beta} A_{RL}^{S*} + S_R^{\beta\alpha} S^{\beta\beta*} A_{RR}^{S*} \right. \\
& - 12 \left(S_L^{\beta\alpha} S^{\beta\beta} A_{LL}^{T*} + S_R^{\beta\alpha} S^{\beta\beta*} A_{RR}^{T*} \right) - 4 \left(S_R^{\beta\alpha} S^{\beta\beta} A_{RL}^{V*} + S_L^{\beta\alpha} S^{\beta\beta*} A_{LR}^{V*} \right) \\
& + 6e^2 \left(S_R^{\beta\alpha} S^{\beta\beta} K_2^{L*} + S_L^{\beta\alpha} S^{\beta\beta*} K_2^{R*} \right) - \frac{36m_\beta}{m_\alpha} \left(S_R^{\beta\alpha} S^{\beta\beta} A_{LL}^{T*} + S_L^{\beta\alpha} S^{\beta\beta*} A_{RR}^{T*} \right) \\
& + \frac{3m_\beta}{2m_\alpha} \left[S^{\beta\beta} \left(11S_L^{\beta\alpha} A_{RL}^{S*} + 2S_R^{\beta\alpha} A_{LL}^{S*} - 7S_R^{\beta\alpha} A_{LR}^{S*} \right) \right. \\
& + S^{\beta\beta*} \left(11S_R^{\beta\alpha} A_{LR}^{S*} + 2S_L^{\beta\alpha} A_{RR}^{S*} - 7S_L^{\beta\alpha} A_{RL}^{S*} \right) \left. \right] \\
& - \frac{6m_\beta}{m_\alpha} \left(S_L^{\beta\alpha} A_{RL}^{S*} - S_R^{\beta\alpha} A_{LR}^{S*} \right) (S^{\beta\beta} - S^{\beta\beta*}) \log \frac{m_\alpha}{m_\beta} \\
& + \frac{12m_\beta}{m_\alpha} \left(S_L^{\beta\alpha} A_{RL}^{V*} - 2S_L^{\beta\alpha} A_{RR}^{V*} + 2S_R^{\beta\alpha} A_{LL}^{V*} - S_R^{\beta\alpha} A_{LR}^{V*} \right) (S^{\beta\beta} - S^{\beta\beta*}) \log \frac{m_\alpha}{m_\beta} \\
& + \frac{3m_\beta}{m_\alpha} \left[S^{\beta\beta} \left(-11S_L^{\beta\alpha} A_{RL}^{V*} + 14S_L^{\beta\alpha} A_{RR}^{V*} - 14S_R^{\beta\alpha} A_{LL}^{V*} + 7S_R^{\beta\alpha} A_{LR}^{V*} \right) \right. \\
& + S^{\beta\beta*} \left(-11S_R^{\beta\alpha} A_{LR}^{V*} + 14S_R^{\beta\alpha} A_{LL}^{V*} - 14S_L^{\beta\alpha} A_{RR}^{V*} + 7S_L^{\beta\alpha} A_{RL}^{V*} \right) \left. \right] \\
& - 4e^2 \frac{m_\beta}{m_\alpha} \left[\left(S_L^{\beta\alpha} K_2^{L*} + S_R^{\beta\alpha} K_2^{R*} \right) (S^{\beta\beta} + S^{\beta\beta*}) \left(6 \log \frac{m_\alpha}{m_\beta} - \frac{21}{2} \right) \right. \\
& + \left. \left(S_L^{\beta\alpha} S^{\beta\beta} K_2^{L*} + S_R^{\beta\alpha} S^{\beta\beta*} K_2^{R*} \right) \left(\pi^2 + 6 \log^2 2 - 6 \log^2 \frac{m_\alpha}{m_\beta} \right) \right] + \text{c.c.} \left. \right\}. \tag{68}
\end{aligned}$$

Replacing Eqs. (60) and (61) into Eq. (68) one finds full agreement with Eq. (65) to order $\mathcal{O}\left(\frac{m_\beta}{m_\alpha}\right)$. This proves explicitly the equivalence between both parametrizations in the calculation of $\ell_\alpha^- \rightarrow \ell_\beta^- \ell_\beta^+ \ell_\beta^-$ mediated by a pure pseudoscalar.

References

- [1] L. Calibbi and G. Signorelli, ‘‘Charged Lepton Flavour Violation: An Experimental and Theoretical Introduction,’’ *Riv. Nuovo Cim.* **41** no. 2, (2018) 71–174, [arXiv:1709.00294 \[hep-ph\]](#).
- [2] **MEG II** Collaboration, A. Baldini *et al.*, ‘‘The design of the MEG II experiment,’’ *Eur. Phys. J. C* **78** no. 5, (2018) 380, [arXiv:1801.04688 \[physics.ins-det\]](#).

- [3] A. Papa, “Towards a new generation of Charged Lepton Flavour Violation searches at the Paul Scherrer Institut: The MEG upgrade and the Mu3e experiment,” *EPJ Web Conf.* **234** (2020) 01011.
- [4] **Mu3e** Collaboration, N. Berger, “The Mu3e Experiment,” *Nucl. Phys. B Proc. Suppl.* **248-250** (2014) 35–40.
- [5] T. Aushev *et al.*, “Physics at Super B Factory,” [arXiv:1002.5012 \[hep-ex\]](#).
- [6] **Belle-II** Collaboration, D. Rodríguez Pérez, “Prospects for τ Lepton Physics at Belle II,” in *17th Conference on Flavor Physics and CP Violation*. 6, 2019. [arXiv:1906.08950 \[hep-ex\]](#).
- [7] **Muon g-2** Collaboration, J. Grange *et al.*, “Muon (g-2) Technical Design Report,” [arXiv:1501.06858 \[physics.ins-det\]](#).
- [8] R. Peccei and H. R. Quinn, “CP Conservation in the Presence of Instantons,” *Phys. Rev. Lett.* **38** (1977) 1440–1443.
- [9] S. Weinberg, “A New Light Boson?,” *Phys. Rev. Lett.* **40** (1978) 223–226.
- [10] F. Wilczek, “Problem of Strong P and T Invariance in the Presence of Instantons,” *Phys. Rev. Lett.* **40** (1978) 279–282.
- [11] L. Di Luzio, M. Giannotti, E. Nardi, and L. Visinelli, “The landscape of QCD axion models,” [arXiv:2003.01100 \[hep-ph\]](#).
- [12] J. Preskill, M. B. Wise, and F. Wilczek, “Cosmology of the Invisible Axion,” *Phys. Lett. B* **120** (1983) 127–132.
- [13] L. Abbott and P. Sikivie, “A Cosmological Bound on the Invisible Axion,” *Phys. Lett. B* **120** (1983) 133–136.
- [14] M. Dine and W. Fischler, “The Not So Harmless Axion,” *Phys. Lett. B* **120** (1983) 137–141.
- [15] F. Wilczek, “Axions and Family Symmetry Breaking,” *Phys. Rev. Lett.* **49** (1982) 1549–1552.
- [16] L. Calibbi, F. Goertz, D. Redigolo, R. Ziegler, and J. Zupan, “Minimal axion model from flavor,” *Phys. Rev. D* **95** no. 9, (2017) 095009, [arXiv:1612.08040 \[hep-ph\]](#).
- [17] Y. Ema, K. Hamaguchi, T. Moroi, and K. Nakayama, “Flaxion: a minimal extension to solve puzzles in the standard model,” *JHEP* **01** (2017) 096, [arXiv:1612.05492 \[hep-ph\]](#).
- [18] S. Centelles Chuliá, C. Döring, W. Rodejohann, and U. J. Saldaña Salazar, “Natural axion model from flavour,” [arXiv:2005.13541 \[hep-ph\]](#).

- [19] M. Reig, J. W. Valle, and F. Wilczek, “SO(3) family symmetry and axions,” *Phys. Rev. D* **98** no. 9, (2018) 095008, [arXiv:1805.08048 \[hep-ph\]](#).
- [20] Y. Chikashige, R. N. Mohapatra, and R. Peccei, “Are There Real Goldstone Bosons Associated with Broken Lepton Number?,” *Phys. Lett. B* **98** (1981) 265–268.
- [21] G. Gelmini and M. Roncadelli, “Left-Handed Neutrino Mass Scale and Spontaneously Broken Lepton Number,” *Phys. Lett. B* **99** (1981) 411–415.
- [22] J. Schechter and J. Valle, “Neutrino Decay and Spontaneous Violation of Lepton Number,” *Phys. Rev. D* **25** (1982) 774.
- [23] C. Aulakh and R. N. Mohapatra, “Neutrino as the Supersymmetric Partner of the Majoron,” *Phys. Lett. B* **119** (1982) 136–140.
- [24] J. Heeck, “Neutrino Lines from Majoron Dark Matter,” *PoS NuFact2017* (2017) 138.
- [25] M. Reig, J. W. Valle, and M. Yamada, “Light majoron cold dark matter from topological defects and the formation of boson stars,” *JCAP* **09** (2019) 029, [arXiv:1905.01287 \[hep-ph\]](#).
- [26] W. Hu, R. Barkana, and A. Gruzinov, “Cold and fuzzy dark matter,” *Phys. Rev. Lett.* **85** (2000) 1158–1161, [arXiv:astro-ph/0003365](#).
- [27] F. Björkeröth, E. J. Chun, and S. F. King, “Flavourful Axion Phenomenology,” *JHEP* **08** (2018) 117, [arXiv:1806.00660 \[hep-ph\]](#).
- [28] F. Björkeröth, L. Di Luzio, F. Mescia, and E. Nardi, “U(1) flavour symmetries as Peccei-Quinn symmetries,” *JHEP* **02** (2019) 133, [arXiv:1811.09637 \[hep-ph\]](#).
- [29] M. Gavela, R. Houtz, P. Quilez, R. Del Rey, and O. Sumensari, “Flavor constraints on electroweak ALP couplings,” *Eur. Phys. J. C* **79** no. 5, (2019) 369, [arXiv:1901.02031 \[hep-ph\]](#).
- [30] M. Bauer, M. Neubert, S. Renner, M. Schnubel, and A. Thamm, “Axion-like particles, lepton-flavor violation and a new explanation of a_μ and a_e ,” *Phys. Rev. Lett.* **124** no. 21, (2020) 211803, [arXiv:1908.00008 \[hep-ph\]](#).
- [31] Q. Bonnefoy, E. Dudas, and S. Pokorski, “Chiral Froggatt-Nielsen models, gauge anomalies and flavourful axions,” *JHEP* **01** (2020) 191, [arXiv:1909.05336 \[hep-ph\]](#).
- [32] C. Cornella, P. Paradisi, and O. Sumensari, “Hunting for ALPs with Lepton Flavor Violation,” *JHEP* **01** (2020) 158, [arXiv:1911.06279 \[hep-ph\]](#).
- [33] J. Albrecht, E. Stamou, R. Ziegler, and R. Zwicky, “Probing flavoured Axions in the Tail of $B_q \rightarrow \mu^+ \mu^-$,” [arXiv:1911.05018 \[hep-ph\]](#).
- [34] J. Martin Camalich, M. Pospelov, H. Vuong, R. Ziegler, and J. Zupan, “Quark Flavor Phenomenology of the QCD Axion,” [arXiv:2002.04623 \[hep-ph\]](#).

- [35] L. Calibbi, D. Redigolo, R. Ziegler, and J. Zupan, “Looking forward to Lepton-flavor-violating ALPs,” [arXiv:2006.04795 \[hep-ph\]](#).
- [36] J. Heeck and H. H. Patel, “Majoron at two loops,” *Phys. Rev. D* **100** no. 9, (2019) 095015, [arXiv:1909.02029 \[hep-ph\]](#).
- [37] W. Porod, F. Staub, and A. Vicente, “A Flavor Kit for BSM models,” *Eur. Phys. J. C* **74** no. 8, (2014) 2992, [arXiv:1405.1434 \[hep-ph\]](#).
- [38] G. Raffelt and A. Weiss, “Red giant bound on the axion - electron coupling revisited,” *Phys. Rev. D* **51** (1995) 1495–1498, [arXiv:hep-ph/9410205](#).
- [39] R. Bollig, W. DeRocco, P. W. Graham, and H.-T. Janka, “Muons in supernovae: implications for the axion-muon coupling,” [arXiv:2005.07141 \[hep-ph\]](#).
- [40] D. Croon, G. Elor, R. K. Leane, and S. D. McDermott, “Supernova Muons: New Constraints on Z' Bosons, Axions, and ALPs,” [arXiv:2006.13942 \[hep-ph\]](#).
- [41] L. Di Luzio, M. Fedele, M. Giannotti, F. Mescia, and E. Nardi, “Solar axions cannot explain the XENON1T excess,” [arXiv:2006.12487 \[hep-ph\]](#).
- [42] M. Giannotti, I. G. Irastorza, J. Redondo, A. Ringwald, and K. Saikawa, “Stellar Recipes for Axion Hunters,” *JCAP* **10** (2017) 010, [arXiv:1708.02111 \[hep-ph\]](#).
- [43] I. M. Bloch, A. Caputo, R. Essig, D. Redigolo, M. Sholapurkar, and T. Volansky, “Exploring New Physics with O(keV) Electron Recoils in Direct Detection Experiments,” [arXiv:2006.14521 \[hep-ph\]](#).
- [44] W. DeRocco, P. W. Graham, and S. Rajendran, “Exploring the robustness of stellar cooling constraints on light particles,” [arXiv:2006.15112 \[hep-ph\]](#).
- [45] E. Masso and J. Redondo, “Compatibility of CAST search with axion-like interpretation of PVLAS results,” *Phys. Rev. Lett.* **97** (2006) 151802, [arXiv:hep-ph/0606163](#).
- [46] **XENON** Collaboration, E. Aprile *et al.*, “Observation of Excess Electronic Recoil Events in XENON1T,” [arXiv:2006.09721 \[hep-ex\]](#).
- [47] A. Djouadi, “The Anatomy of electro-weak symmetry breaking. II. The Higgs bosons in the minimal supersymmetric model,” *Phys. Rept.* **459** (2008) 1–241, [arXiv:hep-ph/0503173](#).
- [48] D. Carmi, A. Falkowski, E. Kuflik, T. Volansky, and J. Zupan, “Higgs After the Discovery: A Status Report,” *JHEP* **10** (2012) 196, [arXiv:1207.1718 \[hep-ph\]](#).
- [49] I. Antoniou, “Constraints on scalar coupling to electromagnetism,” *Grav. Cosmol.* **23** (2017) 171, [arXiv:1508.00985 \[astro-ph.CO\]](#).

- [50] C. Burrage, A.-C. Davis, and D. J. Shaw, “Active Galactic Nuclei Shed Light on Axion-like-Particles,” *Phys. Rev. Lett.* **102** (2009) 201101, [arXiv:0902.2320 \[astro-ph.CO\]](#).
- [51] R. Ballou *et al.*, “Latest Results of the OSQAR Photon Regeneration Experiment for Axion-Like Particle Search,” in *10th Patras Workshop on Axions, WIMPs and WISPs*, pp. 125–130. 2014. [arXiv:1410.2566 \[hep-ex\]](#).
- [52] A. Jodidio *et al.*, “Search for Right-Handed Currents in Muon Decay,” *Phys. Rev. D* **34** (1986) 1967. [Erratum: *Phys.Rev.D* 37, 237 (1988)].
- [53] M. Hirsch, A. Vicente, J. Meyer, and W. Porod, “Majoron emission in muon and tau decays revisited,” *Phys. Rev. D* **79** (2009) 055023, [arXiv:0902.0525 \[hep-ph\]](#). [Erratum: *Phys.Rev.D* 79, 079901 (2009)].
- [54] **TWIST** Collaboration, R. Bayes *et al.*, “Search for two body muon decay signals,” *Phys. Rev. D* **91** no. 5, (2015) 052020, [arXiv:1409.0638 \[hep-ex\]](#).
- [55] **Mu3e** Collaboration, A.-K. Perrevoort, “The Rare and Forbidden: Testing Physics Beyond the Standard Model with Mu3e,” *SciPost Phys. Proc.* **1** (2019) 052, [arXiv:1812.00741 \[hep-ex\]](#).
- [56] A.-K. Perrevoort, *Sensitivity Studies on New Physics in the Mu3e Experiment and Development of Firmware for the Front-End of the Mu3e Pixel Detector*. PhD thesis, Ruprecht-Karls-Universität Heidelberg, 2018.
- [57] **ARGUS** Collaboration, H. Albrecht *et al.*, “A Search for lepton flavor violating decays $\tau \rightarrow e\alpha$, $\tau \rightarrow \mu\alpha$,” *Z. Phys. C* **68** (1995) 25–28.
- [58] E. De La Cruz-Burelo, M. Hernandez-Villanueva, and A. De Yta-Hernandez, “New method for non-standard invisible particle searches in tau lepton decays,” [arXiv:2007.08239 \[hep-ph\]](#).
- [59] **MEG** Collaboration, T. Mori, “Final Results of the MEG Experiment,” *Nuovo Cim. C* **39** no. 4, (2017) 325, [arXiv:1606.08168 \[hep-ex\]](#).
- [60] R. Bolton *et al.*, “Search for the Decay $\mu^+ \rightarrow e^+\gamma$,” *Phys. Rev. Lett.* **56** (1986) 2461–2464.
- [61] J. Goldman *et al.*, “Light Boson Emission in the Decay of the μ^+ ,” *Phys. Rev. D* **36** (1987) 1543–1546.
- [62] R. Bolton *et al.*, “Search for Rare Muon Decays with the Crystal Box Detector,” *Phys. Rev. D* **38** (1988) 2077.
- [63] A. Abada, M. E. Krauss, W. Porod, F. Staub, A. Vicente, and C. Weiland, “Lepton flavor violation in low-scale seesaw models: SUSY and non-SUSY contributions,” *JHEP* **11** (2014) 048, [arXiv:1408.0138 \[hep-ph\]](#).

- [64] A. de Gouvea and P. Vogel, “Lepton Flavor and Number Conservation, and Physics Beyond the Standard Model,” *Prog. Part. Nucl. Phys.* **71** (2013) 75–92, [arXiv:1303.4097 \[hep-ph\]](#).
- [65] T. Aoyama, M. Hayakawa, T. Kinoshita, and M. Nio, “Tenth-Order QED Contribution to the Electron $g-2$ and an Improved Value of the Fine Structure Constant,” *Phys. Rev. Lett.* **109** (2012) 111807, [arXiv:1205.5368 \[hep-ph\]](#).
- [66] T. Aoyama, M. Hayakawa, T. Kinoshita, and M. Nio, “Complete Tenth-Order QED Contribution to the Muon $g-2$,” *Phys. Rev. Lett.* **109** (2012) 111808, [arXiv:1205.5370 \[hep-ph\]](#).
- [67] S. Laporta, “High-precision calculation of the 4-loop contribution to the electron $g-2$ in QED,” *Phys. Lett. B* **772** (2017) 232–238, [arXiv:1704.06996 \[hep-ph\]](#).
- [68] T. Aoyama, T. Kinoshita, and M. Nio, “Revised and Improved Value of the QED Tenth-Order Electron Anomalous Magnetic Moment,” *Phys. Rev. D* **97** no. 3, (2018) 036001, [arXiv:1712.06060 \[hep-ph\]](#).
- [69] **Muon $g-2$ Collaboration**, G. Bennett *et al.*, “Final Report of the Muon E821 Anomalous Magnetic Moment Measurement at BNL,” *Phys. Rev. D* **73** (2006) 072003, [arXiv:hep-ex/0602035](#).
- [70] F. Jegerlehner and A. Nyffeler, “The Muon $g-2$,” *Phys. Rept.* **477** (2009) 1–110, [arXiv:0902.3360 \[hep-ph\]](#).
- [71] **RBC, UKQCD Collaboration**, T. Blum, P. Boyle, V. Gülpers, T. Izubuchi, L. Jin, C. Jung, A. Jüttner, C. Lehner, A. Portelli, and J. Tsang, “Calculation of the hadronic vacuum polarization contribution to the muon anomalous magnetic moment,” *Phys. Rev. Lett.* **121** no. 2, (2018) 022003, [arXiv:1801.07224 \[hep-lat\]](#).
- [72] M. Lindner, M. Platscher, and F. S. Queiroz, “A Call for New Physics : The Muon Anomalous Magnetic Moment and Lepton Flavor Violation,” *Phys. Rept.* **731** (2018) 1–82, [arXiv:1610.06587 \[hep-ph\]](#).
- [73] F. J. Botella, F. Cornet-Gomez, and M. Nebot, “Electron and muon $g - 2$ anomalies in general flavour conserving two Higgs doublets models,” [arXiv:2006.01934 \[hep-ph\]](#).
- [74] S. Gori, G. Perez, and K. Tobioka, “KOTO vs. NA62 Dark Scalar Searches,” [arXiv:2005.05170 \[hep-ph\]](#).
- [75] G. Arcadi, J. Heeck, F. Heizmann, S. Mertens, F. S. Queiroz, W. Rodejohann, M. Sleřák, and K. Valerius, “Tritium beta decay with additional emission of new light bosons,” *JHEP* **01** (2019) 206, [arXiv:1811.03530 \[hep-ph\]](#).
- [76] Y. Uesaka, “Model identification in $\mu^- \rightarrow e^-$ conversion with invisible boson emission using muonic atoms,” [arXiv:2005.07894 \[hep-ph\]](#).

- [77] D. Aristizabal Sierra, M. Tortola, J. Valle, and A. Vicente, “Leptogenesis with a dynamical seesaw scale,” *JCAP* **07** (2014) 052, [arXiv:1405.4706 \[hep-ph\]](#).
- [78] M. G. Folgado and V. Sanz, “On the interpretation of non-resonant phenomena at colliders,” [arXiv:2005.06492 \[hep-ph\]](#).